ACS OMEGA

http://pubs.acs.org/journal/acsodf

Article

# Geological Characteristics and Control Mechanism of Uranium Enrichment in Coal-Bearing Strata in the Yili Basin, Northwest China—Implications for Resource Development and Environmental Protection

Hongyang Bai, Wenfeng Wang,* Qingfeng Lu, Wenlong Wang, Shuo Feng, and Bofei Zhang

Cite This: *ACS Omega* 2022, 7, 5453−5470

Read Online

ACCESS | Metrics & More | Article Recommendations

**ABSTRACT:** Uranium enrichment is considerably prevalent in Jurassic coal-bearing strata in the Yili Basin. A large amount of uranium deposits (occurrences) have been discovered in recent decades. Previous studies have found that uranium deposits and coal seam have a certain correlation in their genesis and spatial distribution or sometimes uranium deposits develop directly in the coal seam. What are the geological characteristics of uranium enrichment? How is uranium enriched? How to strengthen the cooperative development of uranium and coal and environmental protection? In order to explain the aforementioned questions, the characteristics of uranium deposits, rock minerals, and geochemical and metallogenic chronology are summarized herein, and the geological control mechanism of uranium enrichment in coal-bearing strata is discussed. It is found that uranium enrichment (including sandstone uranium deposits and coal uranium deposits) has multistage genetic characteristics and is mainly spread over the gentle slope of the southern margin of the Yili basin, with its host rock possibly being sandstone, coal, and sometimes even mudstone. The uranium concentration has a considerable correlation with the reductant, and the occurrence state of uranium has both inorganic and organic affinities. In addition, uranium enrichment is believed to be a comprehensive effect of high uranium source rocks, tectonic activity, sedimentary facies, hydrogeology conditions, paleoclimate, and reductant. The difference is that uranium enrichment in sandstone is often generated in a mud-sand-mud stratigraphic structure, while uranium enrichment in coal usually develops as coal-sand-mud. What is more, strengthening the study of physical and chemical properties of the host rock, strengthening the study of uranium occurrence state, and sharing geological data are important ways for the cooperative development of coal and uranium resources and environmental protection.

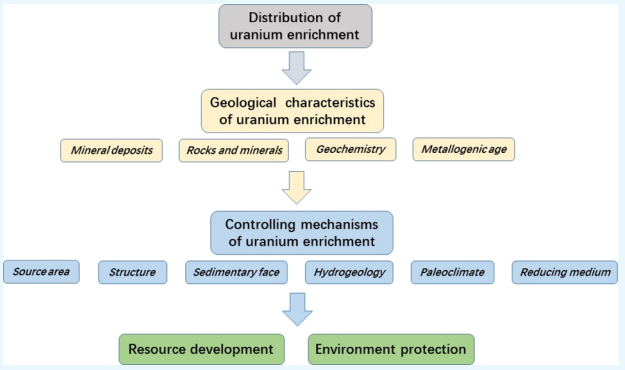


## 1. INTRODUCTION

Both coal and uranium are important energy minerals, whose rational development and clean utilization are of great strategic significance for ensuring the country's energy security as well as for the sustainable and healthy development of the economy. As we all know, coal is the most dominating energy source in China. In 2020, coal consumption has reached 2.8 billion tons, accounting for 56.8% of total energy consumption.[1] At the same time, nuclear power generation came up to 366.243 billion kWh, making up 4.94% of the country's cumulative power generation.[2] The most important source of uranium is sandstone uranium deposits, which are formed in rivers, alluvial fans, and delta regions by injection and replacement methods and then enriched by epigenetic generations.[3] These deposits account for 30% of the world's uranium deposits, but their output can reach nearly half.[4−8] In China, sandstone uranium makes up more than 50% of the total uranium deposits,[9,10] while the Yili basin is the most important uranium-producing basin in Northwest China.[11] There are both sandstone uranium and coal uranium deposits (Table 1) and the resource reserves of the former can reach more than 20,000 tons.[9] In addition, high uranium coal is very common in the coal seams in the Yili basin.

Along with the rapid development of China's economy, contradictions between resource development and environmental protection have gradually emerged in recent years. On

Received: November 30, 2021
Accepted: January 21, 2022
Published: February 3, 2022

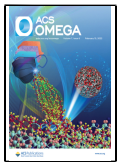

Table 1. Ore-Bearing Strata and Host Rock Types of Main Uranium Deposits in the Yili Basin (from Refs 12 and 14)[a]

| Mineral deposit | | | Honghaigou | Kujieertai (512) | Wukuerqi (513) | Zhajisitan (511) | Mengqiguer (510) | Daladi (509) |
|---|---|---|---|---|---|---|---|---|
| Stratum | | Cycle | Tectonic activity | | | | | |
| | | | Weak | | | | Moderate | Intense |
| Toutunhe | $J_2t$ | $\text{Ⅷ}_2$ | | | | | | |
| | | $\text{Ⅷ}_1$ | | | | | | |
| | $J_2x_3$ | $\text{Ⅶ}_2$ | | | | | | |
| | | $\text{Ⅶ}_1$ | | | | | | |
| Xishanyao | $J_2x_2$ | Ⅵ | | | | | | |
| | $J_2x_1$ | $\text{Ⅴ}_3$ | | | | | | |
| | | $\text{Ⅴ}_2^2$ | | | | | | |
| Sangonghe | $J_1s_2$ | $\text{Ⅴ}_2^1$ | | | | | | |
| | $J_1s_1$ | $\text{Ⅴ}_1$ | | | | | | |
| Badaowan | $J_1b_4$ | Ⅳ | | | | | | |
| | $J_1b_3$ | Ⅲ | | | | | | |
| | $J_1b_2$ | Ⅱ | | | | | | |
| | $J_1b_1$ | Ⅰ | | | | | | |

[a]Note: red, sandstone uranium deposits; black, coal uranium deposits; yellow, both sandstone and coal uranium deposit.

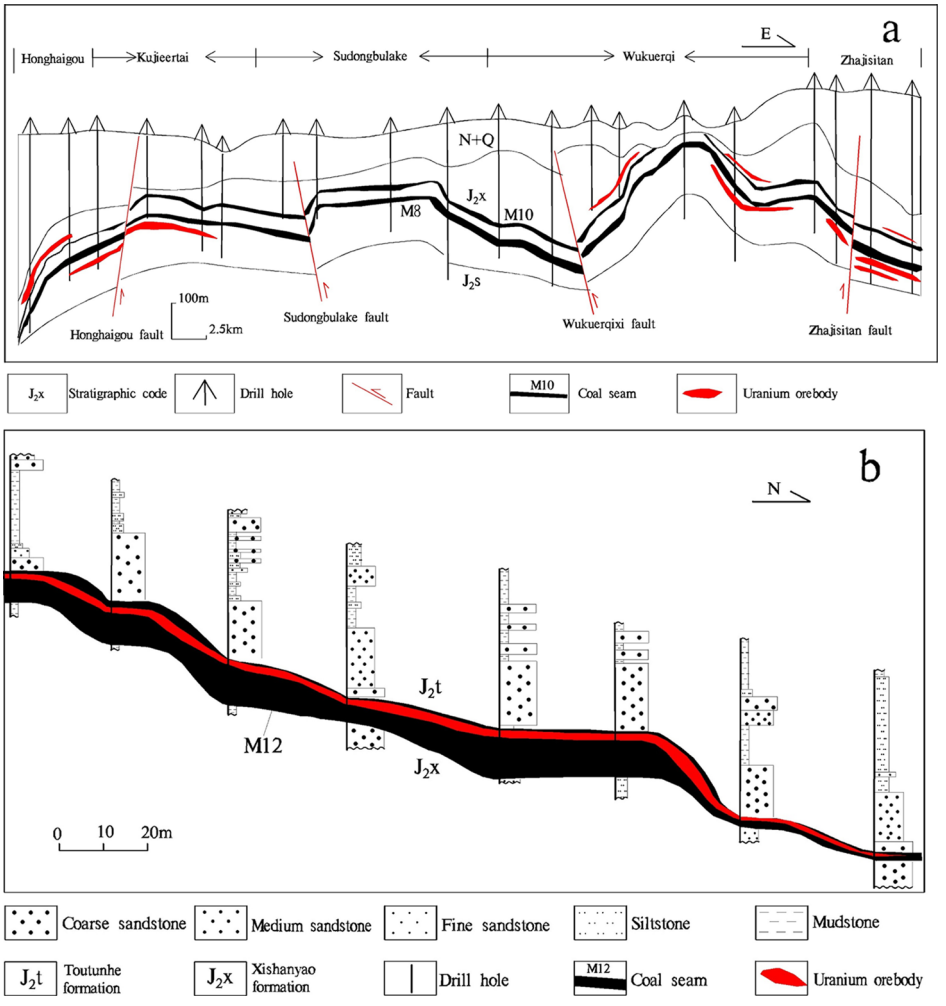


**Figure 1.** (a) Uranium ore body adjoining the coal seam and (b) uranium ore body directly formed in the coal seam (modified from refs 12 and 13).



https://doi.org/10.1021/acsomega.1c06754
ACS Omega 2022, 7, 5453−5470

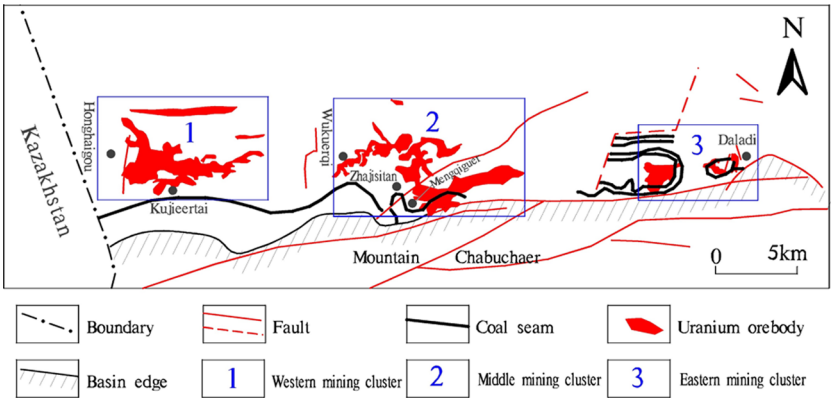


**Figure 2.** Plane distribution of uranium deposits in the southern Yili basin (modified from refs 17−19).

the one hand, a large amount of uranium and coal resources are developed within the Yili basin, and they should be jointly developed and exploited as the energy demand grows. However, due to the fact that these uranium ore bodies are usually adjacent to or directly generated in the coal seam (Figure 1), the joint development of coal and uranium would be a big challenge (if coal is mined first, it will cause damage to the stratigraphic structure, groundwater system, and engineering geological conditions, so uranium resources will be damaged or wasted, which bring dangers to production safety and the ecological environment, and vice versa). Currently, a considerable amount of coal and uranium resources are in a state of restricted mining, considering the dual perspectives of resource development and environmental pollution. It is clear that the enrichment characteristics of uranium in coal-bearing strata are directly related to the clean utilization of coal and the utilization of uranium resources.

Most of the currently known uranium deposits are found in the middle-lower Jurassic Shuixigou group, a set of continental dark coal-bearing clastic rocks, in which uranium deposits and coal seams are often contiguous in terms of spatial output and have a certain connection in genesis. In the southern margin of the basin, three mineral clusters were generated (Figure 2), Honghaigou and Kujieertai (512) in the west, Ukuerqi (513), Mengqiguer (510), and Zhajistan (511) in the middle, as well as Kulustai and Daladi (509) in the east; uranium deposits were spread from the west to east;[14] and a uranium metallogenic belt over a 100 km was formed.[15,16] In the northern basin, a number of uranium enrichment deposits, such as Xinchengzi, Nantaizi, Gangou, Sulu, Piliqing, and Keshanqi, have also been discovered, but most of them are of small size or even just a uranium occurrence. Previous studies were mainly in Chinese and thus with very limited influence, and most of them were conducted solely from the perspective of either sandstone uranium or coal uranium deposits, though the two have rarely been studied as a whole. In this article, the geological characteristics of uranium enrichment (including deposits, rock minerals, and geochemical and metallogenic chronology) are summarized, and the control mechanism of uranium enrichment is discussed, which may bring some enlightenment to resource exploitation and environment protection in the future.

## 2. GEOLOGICAL SETTING

The Yili basin, a relatively closed and stable continental basin with multienergy mineral developed in the middle Tianshan orogenic belt,[20−22] is tectonically situated on the Yili microblock in the south-eastern Kazakhstan plate[23−35] (Figure 3). To the north and the south of the basin is mount Chabuchar and mount Keguqin, respectively.[36−42] On Mount Keguqin, Proterozoic metamorphic sedimentary rocks, Carboniferous volcanoes and pyroclastic rocks, Permian granites are exposed,[43] among which Permian granites and Carboniferous acidic volcanic and pyroclastic rocks are variably enriched in uranium and may be the main source of uranium in the basin.[38,44−51]

The basin has experienced intense uplifts in the intra-arc basin (P1), the intra-arc residual basin (P2), the Mesozoic and Cenozoic pelagic collision mountain basin and the Neogene Tianshan orogenic belt,[52−54] as a result, is divided into the northern (a fold uplift area) and southern (a deep depression area) parts by the Huocheng-Tuokai fault. Vertically, the basin is composed of the meso-new Proterozoic crystalline basement, the late Paleozoic volcanic rock transition layer and Mesozoic−Cenozoic sedimentary caprock. The lower Triassic is missing in the basin, and a set of fluvial-lacustrine clastic rocks were deposited in the middle-late Triassic. The deposition center is located in the Chabuchaer County and Yining City. In the Jurassic, the deposition center moved north to Huocheng and Yining County, the lower middle Jurassic was a set of fluvial and lacustrine facies coal-bearing clastic rocks, while lower Cretaceous was generally missing. The Cenozoic is dominated by fluvial alluvial fan facies.[53−55]

The Jurassic strata (Figure 4) in the basin are the most important coal-bearing strata, mainly developed in the middle and lower Jurassic Shuixigou Group and the overlying Toutunhe formation. The former, most widely distributed in the basin, is a set of mainly gray continental coal-bearing clastic rock series that is characterized by interbedded sandstone and mudstone interbedded with coal seams (or lines), stable 5th, 8th, and 10th coal seams[12] and non-coal rocks always contain a lot of carbon chips and pyrite. The sandstone is dominated by feldspar lithic sandstone or lithic sandstone, with poor cementation and a loose texture.[12,40,55,56] Almost all spores and pollen are fern spores and gymnosperm pollen, showing that they were generated in a warm and humid climate.[55,57]

The Shuixigou group, whose total thickness is 300−1142 m (with the largest thickness in the center of the basin, followed by the north, and thinner in the south), consists of the Badaowan formation, Sangonghe formation, and Xishanyao formation from the bottom to the top, respectively.[58] This set of strata has attracted much attention due to the large number of uranium resources,[36,53−55] and a series of uranium deposits have been discovered in the southern margin of the basin. Uranium ore


https://doi.org/10.1021/acsomega.1c06754
ACS Omega 2022, 7, 5453−5470

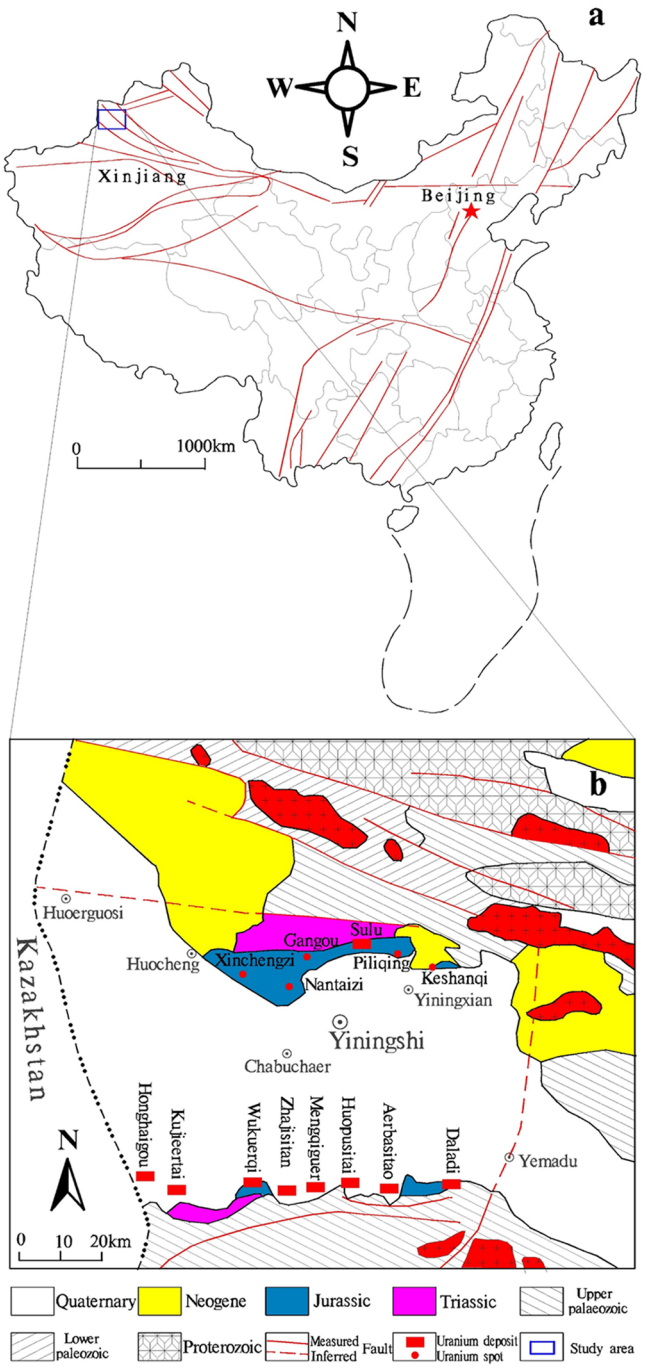


**Figure 3.** (a) Location and (b) geological sketch map of the Yili Basin (modified from ref 44).

isotope dating results show that the mineralization period is mainly concentrated in the middle and Pliocene.[59] In addition, some uranium ore body has also been found in the overlying Toutunhe, the high uranium value areas were mainly distributed in the turmeric glutenite above the coal seam. Uranium was abnormally prominent in the interface between the coal seam and conglomerate (or glutenite and sandstone).

## 3. RESULTS AND DISCUSSION

**3.1. Geological Characteristics of Uranium Enrichment.** *3.1.1. Mineral Deposits.* Varying degrees of uranium mineralization are discovered in almost all of the stratum of the Shuixigou Group (Table 2), and whose host rocks include sandstone and coal. Sandstone uranium deposits are mainly developed in the middle of the southern margin of the basin in cycle V, followed by cycle VII, while the ore bodies are always located at the transitional or changing part of terrain, stratum thickness, and lithology (e.g., the terrain from steep to slow, lithology from coarse to fine). These ore bodies are mainly of curl and imbricate (Figure 5) in the section, and advances into the basin with the development of the interlayer oxidation zone,[60] which are mostly characterized by medium to coarse grains, loose structure, and gentle occurrence.

Coal uranium deposits mainly developed in Honghaigou mining in the west, the Daladi mining in the east, and some small scale in Zhajisitan and Mengqiguer in the central of the southern margin of the basin. Among them, Honghaigou is the most special one, with its ore bodies mainly present in cycles VII and VIII (differing from other mining areas), which maybe contributed to the joint influence of the structure and the interlayer oxidation zone. There are many uranium-bearing coal seams in Daladi mining, where uranium mineralization is developed in almost every coal seam to varying degrees. However, the ore bodies are thin and localized on the whole, which is probably related to the migration conditions of uranium-bearing fluid due to strong tectonic activity and excessive change of the stratigraphic dip angle in the east of the southern margin of the basin.[13,14,18,19,61,62]

*3.1.2. Rocks and Minerals.* The ore-bearing sandstone of the Shuixigou Group is mainly lithic sandstone (Figure 6), less lithic quartz sandstone, and a small amount of quartz sandstone. Most of the debris has poor roundness, angular sub-circular, and their contact is dominated by dots and lines. The main clastic components are quartz (30−40%), feldspar (15−20%), and rock cuttings (20−40%) (Min et al., 2005a) and varying degrees of carbon chips and asphalt.[55] Among them, epigenetic enlargement can be seen in quartz chips. The cuttings mainly include rhyolite lava, tuff, granite, siliceous rock, flint, quartz schist, quartz mica schist, sandstone, slate, and so forth (acidic igneous rock cuttings account for about 25.6−28.3%). The interstitial material accounts for about 7−16.33%, which is mainly composed of heterophylls (>90%) and a little cement (<10%). The matrix is dominated by kaolinite, which may be related to the interaction between aluminosilicate minerals prevalent in sandstone and acidic reducing liquid of coal-bearing rock series. The main clastic composition of the uranium ore is not significantly different from that of the original rock, but the development of particulate pyrite, uranium mineral pitch uranium, or uranium stone, and so forth indicates that they were formed in the same or similar paleogeological-geographical depositional environment.[32,43,55]

Ore-bearing coal is mainly lignite-low rank bituminous characterized by high-moisture, low-ash, and medium−high sulfur, with a loose structure and friability (Figure 7). The macroscopic coal rock type is semi-dark−semi-bright coal, with dark coal as the main component, followed by bright coal. Dark coal is mostly strip-shaped and bright coal and vitrinite are mostly lenticular. The inertinite components are significantly higher than that of the vitrinite, and the exinite is very rare. The content of inertinite has a significant increase from bottom to top, and the vitrinite group is just the opposite. Uranium occurs mainly in minerals and dispersed adsorption. Uranium minerals include bituminous uranium (usually in the form of individual particles smaller than 0.01 mm) and uranium black. Most of the bituminous uranium is filled in the cracks of the coal in the form of fine veins. Dispersed adsorption uranium is the main form of


https://doi.org/10.1021/acsomega.1c06754
ACS Omega 2022, 7, 5453−5470

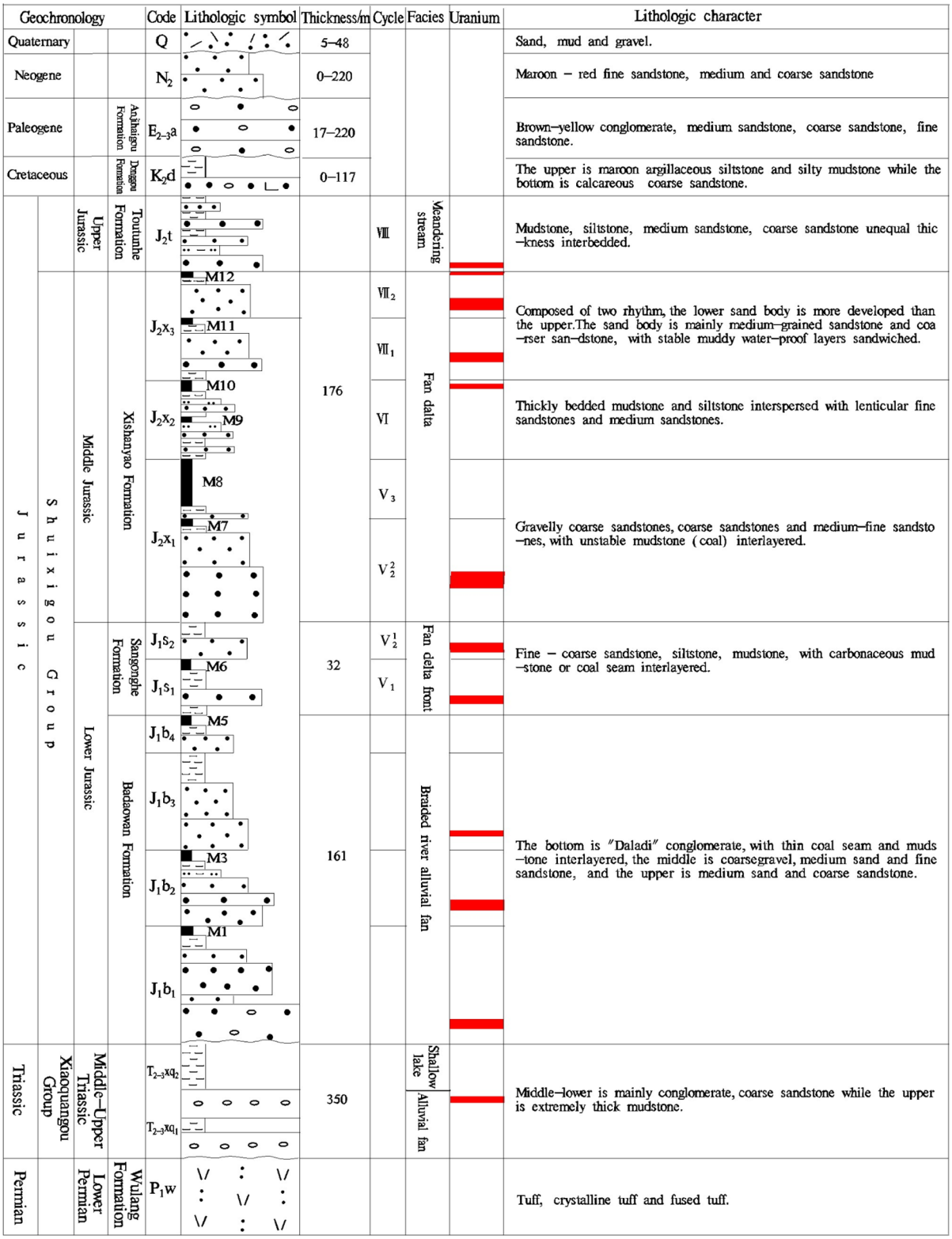


**Figure 4.** Stratigraphic column for the sedimentary cover in the southern Yili basin (modified from ref 12).

uranium in coal, accounting for about 80%, and is mainly adsorbed by coal, organic carbon, plant remains, mudstone, and so forth.[62]

*3.1.3. Geochemistry.* The water–rock reaction that occurs during the migration of uranium-oxygenated water will inevitably change the physical and chemical conditions of the medium[67,68] and thus is reflected in the elements. The major elements in the ore-bearing sandstone (compared to the original rock) have the characteristics of high silicon and low sodium, which may be related to the clayization of feldspar minerals and thus causes the loss of alkali metals, and the formation of amorphous $SiO_2$, $Al_2O_3$, and $TFe_2O_3$ is of high activity (Table 3). The content of $SiO_2$ is significantly increased from the oxide sub-zone to the uranium ore sub-zone, while $Al_2O_3$ and $TFe_2O_3$


https://doi.org/10.1021/acsomega.1c06754
ACS Omega 2022, 7, 5453–5470

**Table 2. Scale and Grade of Main Uranium Ore Bodies in the Yili basin**

| mineral deposit | host rock | straum/cycle | length (m) | width | thickness (m) | grade (%) | reference |
|---|---|---|---|---|---|---|---|
| Honghaigou | sandstone | VII−VIII | | | 25−30 | | 18, 19 |
| | | M12 | | | 0.4−2.4 | 0.0503−0.5720 | 13, 18, 19 |
| Kujieertai (512) | sandstone | V | 5300 | 250−850 | 0.1−12.3 | 0.01−1.5 | 14, 20, 21 |
| Wukuerqi (513) | sandstone | V | | | 0.45−7.45 | 0.017−0.095 | 63 |
| Zhajisitan (511) | sandstone | V | 2800 | 100−600 | 6−13, 0.1−3.5 | 0.0129−0.1364 | 53, 54 |
| Mengqiguer (510) | sandstone | V2-2 | 1500 | 50−400 | 3−9 | 0.0339−0.3498 | 64 |
| Daladi (509) | coal | M1, M9, M10 | ∼206 | | 0.55−2.62 | ∼0.279 | 62 |

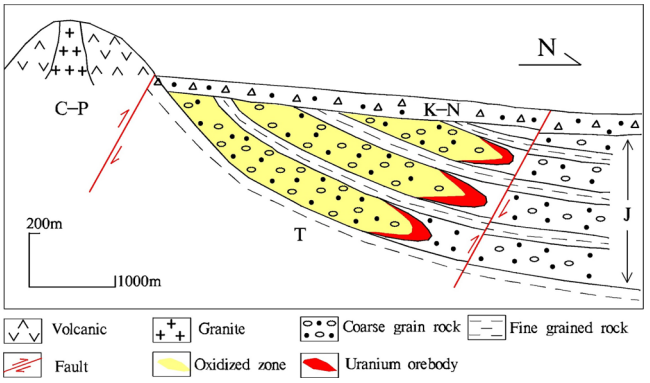


**Figure 5.** Morphology of uranium ore bodies in the Yili basin (modified from ref 39).


**Figure 7.** Macroscopic characteristics of the Honghaigou rock core in the Yili basin: (a) strong oxidation sandstone, red; (b) oxidation sandstone, yellow, (c) gray-white ore-bearing sandstone, underlying ore-bearing coal seam; (d) reductive siltstone, dark gray; and (e) ore-bearing coal seam, broken.

decrease. CaO, MgO, $K_2O$, and $Na_2O$ are of general activity and are related to the variation of PH. $MnO_2$, $TiO_2$, and $P_2O_5$ are of the worst activity, which may be related to the heavy minerals in coal.

In addition, organic carbon and sulfide are positively correlated with the content of U, gradually increasing from the oxidation zone to the primary rock zone, and reach the highest in the transition zone. The trace elements Se, Re, Ga, V, Ge, and Mo are all enriched in different degrees and generally have the highest content in the transition zone of the interlayer oxidation zone, showing similar geochemical behavior to U. Among them, Se, Re, and Ga have reached the level of comprehensive utilization.

The total content of rare earth elements (∑REE) generally have a trend of low-high-low from the strong oxidation zone to the reduction zone (transition zone reach the highest), indicating that the ∑REE in the interlayer oxidation zone-oxidized sandstone is depleted. That is, ∑REE was lost during the process of interfluid migration, and then sedimentation and enrichment in the transition zone. The enrichment of uranium can be divided into two stages as follows: a pre-enrichment in the formation of ore-bearing host rock, for example, the uranium background values in the Kujiertai mining area V, II (I−II), and VII cycle rocks are the highest (more than 5 ppm), while the Th/

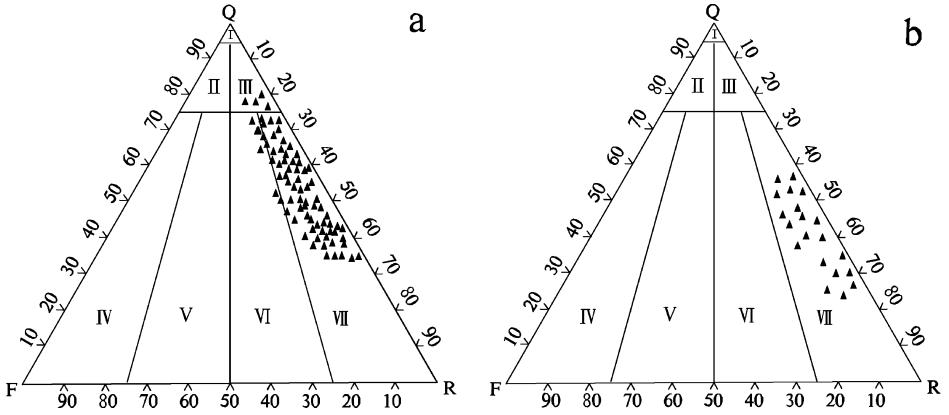


**Figure 6.** (a) Sandstone types of Shuixigou group in Suasugou and (b) and Toutunhe formation in Honghaigou, southern margin of the Yili basin (I, quartz sandstone; II, feldspar quartz sandstone; III, lithic quartz sandstone; IV, arkose; V, lithic feldspar sandstone; VI, feldspar lithic sandstone; and VII, lithic sandstone) (modified from refs 65 and 66).



https://doi.org/10.1021/acsomega.1c06754
ACS Omega 2022, 7, 5453−5470

**Table 3. Major Elemental Contents in the Ore-Bearing Interstratified Oxidized Zone Kujieertai Uranium Deposit (from Refs 20 and 21)[a]**

| | complete oxidation sub-zone | incomplete oxidation sub-zone | local oxidation sub-zone | acidification front sub-zone | uranium ore sub-zone | original rock |
|---|---|---|---|---|---|---|
| $SiO_2$ | 4.34(−5.52) | 77.01(−2.85) | 80.76(+0.90) | 86.03(+6.17) | 81.84(+1.98) | 79.86 |
| $Al_2O_3$ | 11.94(+2.64) | 11.02(+1.72) | 9.14(−0.16) | 7.04(−2.26) | 8.20(−1.10) | 9.3 |
| $TFe_2O_3$ | 2.73(+1.27) | 2.44(+0.98) | 1.36(−0.10) | 0.82(−0.64) | 1.27(−0.19) | 1.46 |
| CaO | 1.69(+1.42) | 0.39(+0.12) | 0.24(−0.03) | 0.19(−0.08) | 0.34(+0.07) | 0.27 |
| MgO | 0.55(−0.21) | 0.66(−0.10) | 0.59(−0.17) | 0.48(−0.28) | 0.41(−0.36) | 0.76 |
| MnO | 0.06(0.00) | 0.02(−0.04) | 0.03(−0.03) | 0.03(−0.03) | 0.01(−0.05) | 0.06 |
| $TiO_2$ | 0.50(+0.14) | 0.35(−0.01) | 0.36(0.00) | 0.32(−0.04) | 0.40(+0.04) | 0.36 |
| $P_2O_5$ | 0.08(+0.02) | 0.08(+0.02) | 0.07(+0.01) | 0.06(0.00) | 0.04(−0.02) | 0.06 |
| $K_2O$ | 2.61(+0.18) | 2.60(+0.17) | 2.33(−0.10) | 2.20(−0.23) | 2.16(−0.27) | 2.43 |
| $Na_2O$ | 0.46(+0.13) | 0.39(+0.06) | 0.60(+0.27) | 0.14(−0.19) | 0.67(+0.34) | 0.33 |
| FeO | 0.27 | 0.76 | 0.5 | 0.38 | 0.9 | 0.72 |
| $Fe_2O_3$ | 2.43 | 1.61 | 0.8 | 0.4 | 0.27 | 0.59 |
| $Fe^{3+}/Fe^{2+}$ | >3.5 | 3.5−2.0 | 2.0−1.1 | 1.1−0.9 | <0.74 | 0.74 |

[a]Note: in parentheses is the difference from the original rock.

**Table 4. Uranium Background Concentration and Th/U of Some Deposits in the Yili Basin (from Ref 15)**

| | Kujieertai | | | Wukuerqi | | | Zhajisitan | | |
|---|---|---|---|---|---|---|---|---|---|
| | U | Th/U | SQ[a] | U | Th/U | SQ | U | Th/U | SQ |
| I | 5.9 | 1.3 | 34 | 5.2 | 2.79 | 2 | 3.22 | 2.19 | 10 |
| II | 5.06 | 1.34 | 30 | | | | 4.82 | 1.26 | 18 |
| III | 4.19 | 1.38 | 32 | | | | 3.86 | 1.49 | 18 |
| IV | 3.6 | 1.9 | 81 | 1.9 | 3.16 | 2 | 3.75 | 1.4 | 28 |
| V | 5.85 | 1.76 | 300 | 6.58 | 0.9 | 52 | 5.71 | 1.55 | 114 |
| VI | 3.99 | 3.08 | 139 | 4.9 | 1.46 | 14 | 3.65 | 2.98 | 12 |
| VII | 4.72 | 2.29 | 101 | 7.14 | 1.52 | 15 | 4.54 | 2.25 | 23 |
| VIII | 1.61 | 4.55 | 11 | | | | 4.15 | 2.14 | 13 |

[a]Note: SQ is short for sample quantity.

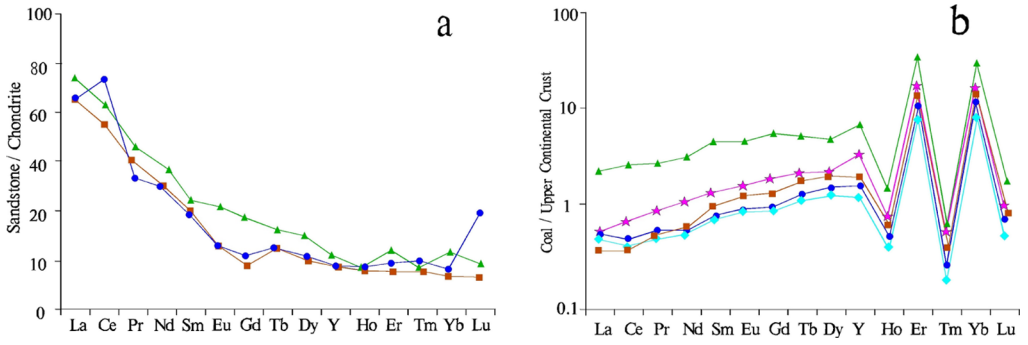


**Figure 8.** REE distribution patterns of (a) sandstone (modified from ref 69) and (b) coal in the Yili basin.

**Table 5. Relationship between the Metallogenic Age and the Uranium Grade in the Yili Basin (from Ref 59)**

| uranium concentration (ppm) | average age (Ma) | sample quantity |
|---|---|---|
| ≥1 | 3.5 | 8 |
| 0.05−1 | 7.1 | 13 |
| 0.01−0.05 | 11.4 | 12 |
| 0.002−0.01 | 60.5 | 16 |
| 0.001−0.002 | 84.2 | 11 |

U ratio is lower than the adjacent cycles (Table 4). At the same time, cycles V and VII are an important bed of uranium mineralization;[15] the second stage is the transformation mineralization of epigenetic uranium oxidized water.

The element content of the uranium-rich coal is C (60−70%), H (3−5%), O (16−25%), N (0.7−1.3%), and S (0.6−5%),[62] which has medium-high sulfur in comparison with raw coal. In terms of trace elements, the coal is enriched in U (maximum 7207 μg/g), Se (maximum 7207 μg/g), Mo (maximum 1248 μg/g), Re (maximum 34 μg/g), As (maximum 234 μg/g), and Hg (maximum 3858 ng/g),[70] among which Se and Mo are positively correlated with U, and enriched in uranium industrial deposits. Selenium occurs in natural selenium, with an average grade of 0.044%. In addition, rare earth elements (∑REE) in coal have the characteristics of heavy or medium enrichment compared with sandstone (Figure 8). Dai et al.[70] and Yang[71] attributed the above-mentioned abnormality to the chemical composition of the source rock and the penetration of the two



https://doi.org/10.1021/acsomega.1c06754
ACS Omega 2022, 7, 5453−5470

Table 6. Metallogenic Ages of Uranium Deposits in the Southern Margin of the Yili Basin (from Refs 4 and 76)

| Mineral area | Age(Ma) | | | | | | | | |
|---|---|---|---|---|---|---|---|---|---|
| | J | K | E1 | E2 | E3 | N1 | N2 | Qp | Qh |
| Honghaigou | | | | | | | | 0.6 | |
| Kujieertai (512) | | 108～69 | | 51～25 | | 19,12～3 | | 2～0.7 | |
| Wukuerqi (513) | | | | | | 12～2 | | | |
| Zhajisitan (511) | | | | | 60.5～30、25～15、12～0.3 | | | | |
| Mengqiguer(510) | 158～153 | 82 | 55 | | 28.3～12.1,9.2～5.1,3.8～2.6,1.38～0.22,0 | | | | |
| Daladi (509) | | | | | | 7.8～5.5 | | | |

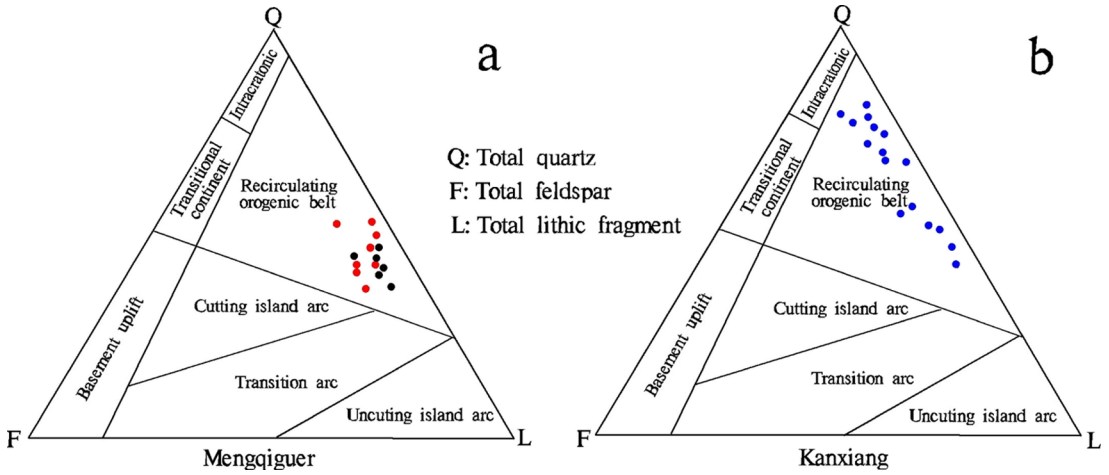


Figure 9. Dickinson diagram of sandstone components of Shuixigou Group in (a) Mengqiguer and (b) Kanxiang, southern Yili basin (modified from refs 65 83, and 84).

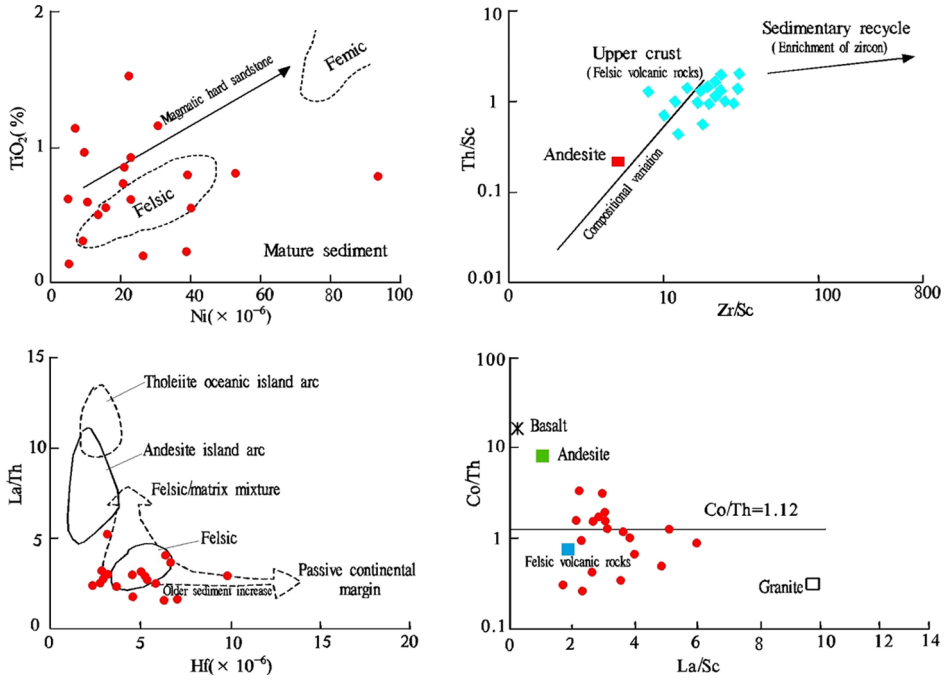


Figure 10. Discrimination diagram of the clastic rock source region of middle and lower Jurassic in the southern margin of the Yili basin (modified from ref 85).

phases of U−Se−Mo−Re-rich and Hg−As-rich epithermal fluids.

As for the occurrence state of uranium, the studies are relatively limited. In spite of this, the independent uranium minerals such as pitchblende, coffinite, and uranite and some



https://doi.org/10.1021/acsomega.1c06754
ACS Omega 2022, 7, 5453−5470

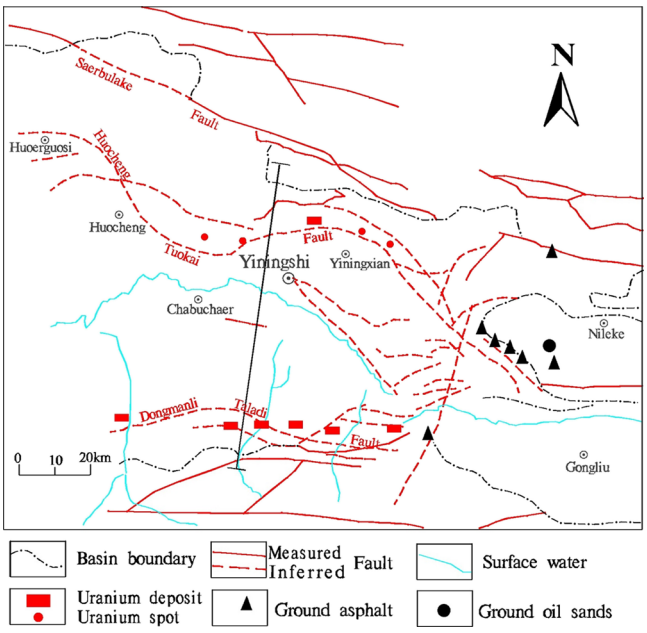


**Figure 11.** Distribution of structures, main uranium deposits, and surface oil seedlings (modified from ref 22).

other uranium-bearing minerals are usually common in the sandstone uranium deposit. In addition, the uranium content in the ore body is obviously related to the organic carbon and sulfur contents, indicating that uranium may exist in an organic state.[18,19,59,72] That is to say, there are both inorganic affinity and organic affinity of uranium. Dai et al. observed pitchblende and coffinite and other uranium-bearing minerals filled in the cavity of inertinite in coal. Meanwhile, the observation of vitrinite indicated that uranium enrichment in coal may be related to organic components.[70]

*3.1.4. Metallogenic Age.* Field observation and mineral identification show that uranium mineralization occurred long after the deposition of the Shuixigou group and are a multistage mineralization process.[32,43,58] However, the mineralization age is inversely proportional to the uranium concentration of the ore (Table 5). In previous studies, most were conducted with uranium-lead isotope isochron and apatite fission track thermochronology (AFTT), for example, U−Pb dating of sandstones and uranium ore from Zhajisitan, secondary ion mass spectroscopy (SIMS) analysis, and U−Pb dating of pitchblende from Mengqiguer, U−Pb dating and AFTT of the uranium ore from Daladi uranium and so forth.,[59,72−75] which showed that uranium mineralization has mainly occurred since the Miocene and has been occurring even up to the present time (Table 6), for example, 11.7 ± 0.3 to 15.8 ± 0.4, 5 ± 1, 2 ± 0,[59,75] and 0.61 ± 0.2−0.347 ± 0.0048 Ma,[4] which was consistent with the Himalayan movement in northwest China.

**3.2. Mechanism of Geological Control.** *3.2.1. Source Area.* The detrital quartz in the host sandstone is mainly single-crystal quartz with non-wavy extinction, while the feldspar consists mainly of potassium feldspar, which indicates that the parent rock originated from the volcanic rock source area. At the same time, the Dickinson diagram reveals that the clastic rocks were formed in a cyclic orogenic environment (Figure 9). The composition of the main debris is complex, but the igneous rock debris is found in different degrees, and the intermediate acid volcanic rock debris accounts for nearly 1/3 of the total debris. From west to east, the igneous rock debris gradually varies from basic and intermediate acid combination to a single intermediate acid volcanic rock.[15]

Meanwhile, the ratio or content of some indicator elements in fine-grained clastic rocks can effectively reflect the compositional characteristics of the parent rocks in the source region.[77,78] The $Al_2O_3/TiO_2$, Ni-$Tio_2$, Cr/Zr, La/Th−Hf, Zr/Sc, and Th/Sc as well as the ∑REE distribution patterns and Eu negative anomaly of mudstone and siltstone in the mining area, as shown in Figure 10, suggest a source of intermediate acid volcanic rocks and sedimentary rocks derived from granite.[78−82]

In addition, detrital zircon geochronology shows a provenance of early-middle Permian-Carboniferous rocks and the newer the age, the greater the contribution of Devonian and Silurian, indicating that the provenance denudation in the Jurassic was characterized by unroofing.[65,79]

In summary, the detrital characteristics, zircon age characteristics, and element geochemical characteristics all indicate that the detrital originated from the orogenic belt of recycling, and the parent rocks were mainly a medium acid volcanic sedimentary rock series formed in the Carboniferous continental island arc.

*3.2.2. Structure.* Two longitudinal anticlines, Kujieertai and Wukuerqi, were formed on the basis of the monoclinal structure in the southern basin, and the consequent uplift provided sufficient power for the migration and convergence of U-bearing

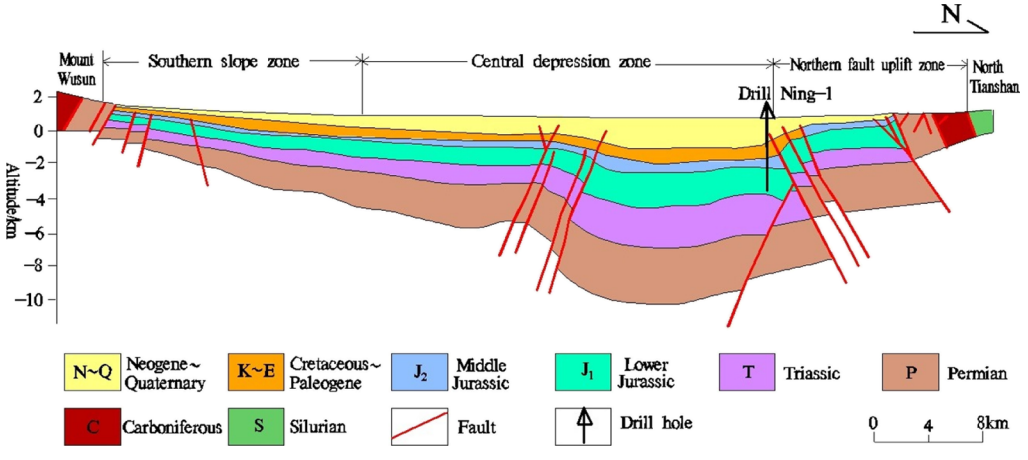


**Figure 12.** Section of Figure 11 (modified from ref 22).



https://doi.org/10.1021/acsomega.1c06754
ACS Omega 2022, 7, 5453−5470

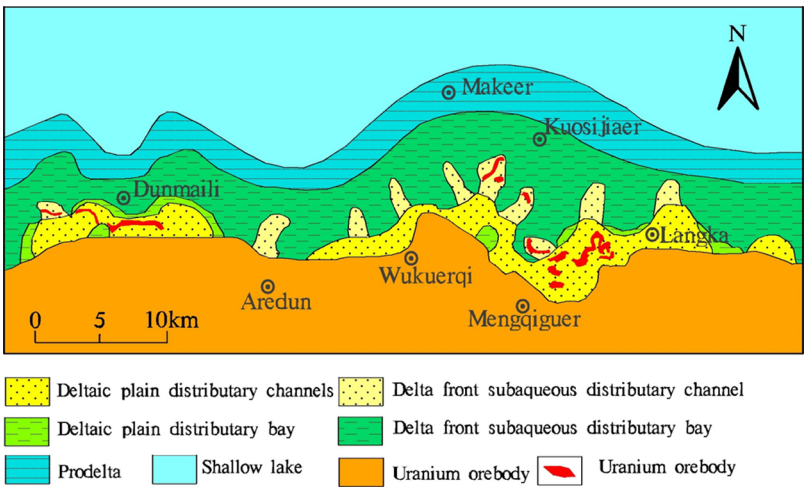


**Figure 13.** Relationship between sedimentary facies and uranium mineralization of lower Xishanyao formation in the southern margin of the Yili basin (modified from ref 86).

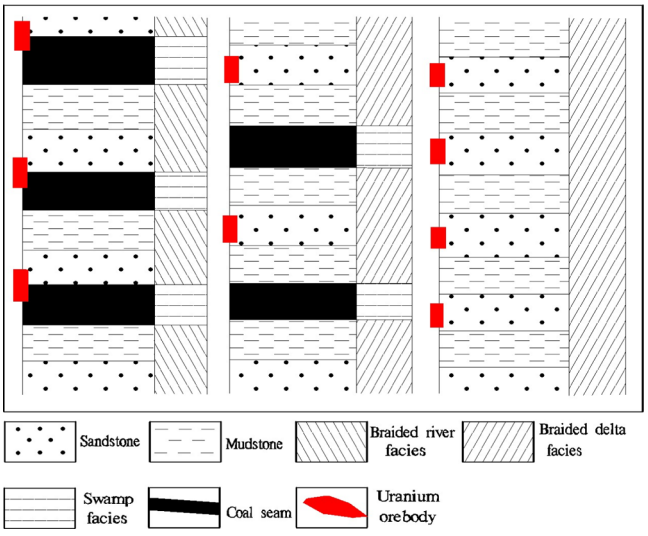


**Figure 14.** Lithology and lithofacies' sequence of ore-bearing strata in the Yili basin (modified from ref 87).

fluid. In other words, tectonic activity controlled the groundwater recharge−runoff−discharge system, leading to the structural transition zone becoming a favorable metallogenic area.[18,19]

It is well known that tectonic fault zones are important channels for the migration of the reductant in uranium enrichment and precipitation. The uranium deposits (points) discovered in the basin have a good coupling with the deep and large faults, ground bitumen, and oil sand (Figure 11). Uranium deposits (points) in the northern margin of the basin are mainly distributed near the Huochengtuokai fault and in the southern margin are roughly located near the Dongmanli-Daladi fault, which could be attributed to the upward trend of the oil and gas along the two large faults resulting in the formation of strong reduction barriers as well as the reduction, precipitation, and enrichment of uranium.[22]

In addition, tectonic activity formed the provenance of high uranium rocks (Figure 12): a large number of the continental island arc volcanic rocks were developed in the southern margin of the Yili-Central Tianshan block during the late Devonian to late Carboniferous subduction of the Southern Tianshan ocean. At the end of the Late Carboniferous, the Yili-Central Tianshan block collided with the Tarim block and formed a large amount of volcanic-clastic rocks, thus forming the provenance area with high uranium concentrations.[22]

What is more, tectonic activity on basin sedimentation directly affects the development of ore-bearing host rocks. In the early Jurassic, the rapid uplift of the southern margin of the basin caused the Carboniferous and Permian volcanic sedimentary strata to be uplifted and denuded, resulting in a large drop between the mountain and the basin and the rapid filling of the basin by coarse debris, forming the fan delta deposits of Badaowan formation. At the end of the early Jurassic, lacustrine deposits of the Sangonghe formation were formed due to the rapid expansion of the lake basin, rising of the lake level, and insufficient supply of the sediment. After the middle Jurassic, due to the dual influence of the denudation of the mountain and the filling of the basin, the relative elevation difference between the mountain and the basin was constantly reduced and the lake level was constantly shrinking until it disappeared, forming the braided river delta deposition of the Xishanyao formation and fluvial facies deposition of the Toutunhe formation.[52,65] In addition, stable subsidence during the coal accumulation period and relatively stable slow uplift tectonic movement after coal accumulation provide a favorable tectonic environment for coal seam preservation and uranium enrichment.[17,26]

*3.2.3. Sedimentary Face.* To the sandstone uranium deposit, the braided river delta (borehole ore yield 63.9%) is the most favorable metallogenic system, followed by the fan-braided river sedimentary system (borehole ore yield 22.2%) and meandering river delta sedimentary system (borehole ore yield 13.9%)[22,86] (Figure 13). The thickness of sand bodies is usually stable and strictly restricts the development of the interlayer oxidation zone. The uranium ore body is usually located at the place where the thickness of the sand body decreases or the boundary between the sand body and mudstone (or coal). The strata structure is always made of mud-sand-mud or mud-sand-mud-coal (Figure 14) and the ore-bearing sandstones are mainly medium coarse grains with loose cementation, good porosity, and permeability.

In the river flood basin, the edge beach sedimentary sand body mainly overlies the coal seam directly, which is a typical bottom scour structure. The oxidation degree of the sand body is enhanced, which makes the transition subzone of the interlayer


https://doi.org/10.1021/acsomega.1c06754
ACS Omega 2022, 7, 5453−5470

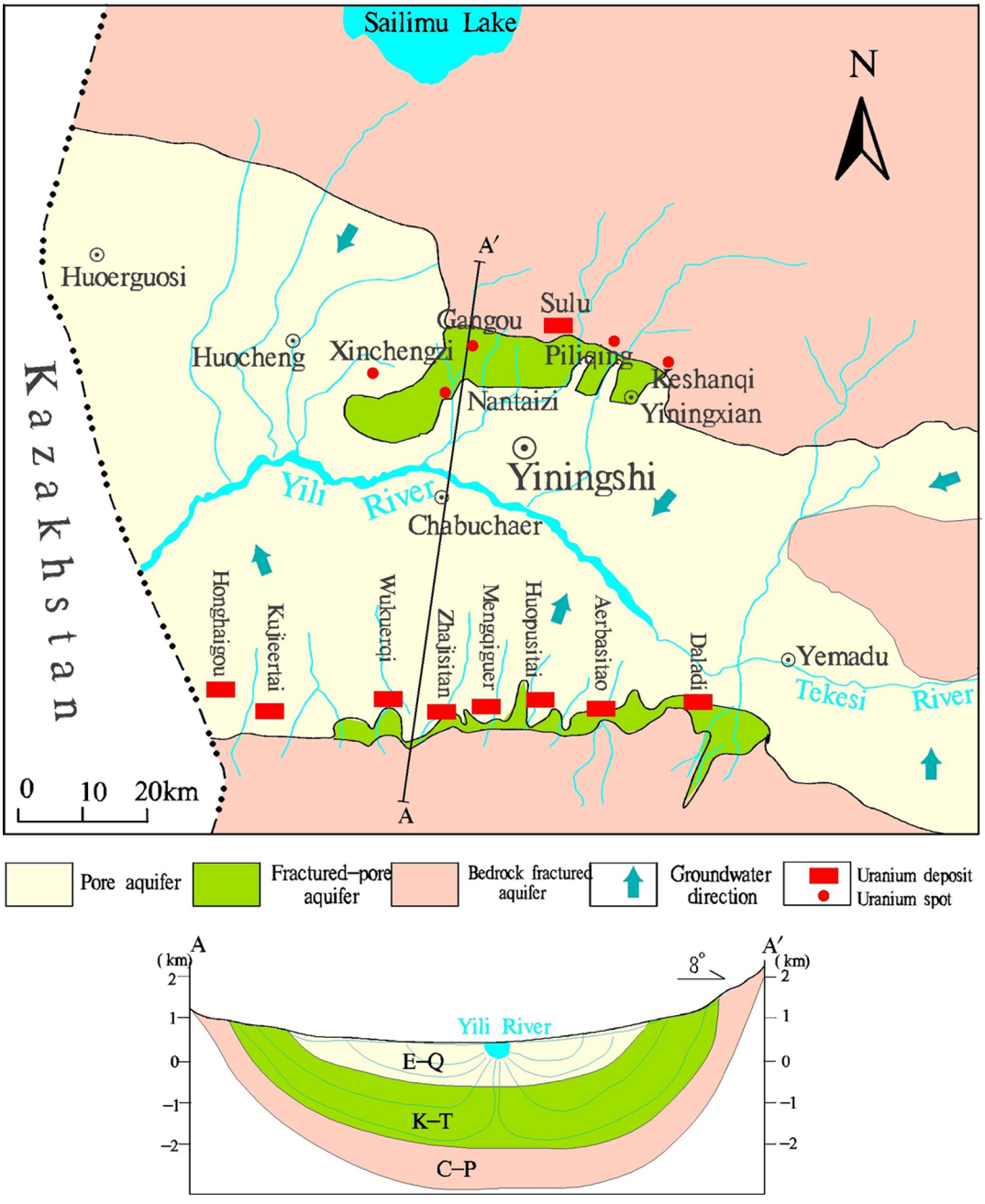


**Figure 15.** Hydrogeological sketch of the Yili Basin (modified from ref 88).

oxidation zone move downward. At the same time, the upward migration of carboxylic acid and $CO_2$ formed by erosion and organic matter evolution in the upper coal seam are often loose and porous, greatly improving the permeability, and thus becoming a good reservoir.

In addition, the fore-lake and back-lake swamps of fan-braided river alternate many times, which easily form the sand–coal–clay structure (Figure 14). Under the action of an oxygen-bearing interlayer fluid for a long time, the interlayer sand bodies are mostly completely oxidized (destruction of the earlier sand body uranium mineralization). Meanwhile, the underlying coal seam develops the ore body because of its good adsorption and reduction for uranium.

*3.2.4. Hydrogeological Conditions.* The hydrogeochemical cycle is the main form of the uranium cycle, and the suitable recharge, runoff, and discharge system are the basic conditions for uranium enrichment. The mountainous slope zone in the southern basin can widely receive the recharge of surface water, atmospheric precipitation, and snow melt water and increases the hydraulic gradient, the coarse-grained sand bodies developed in the Shuixigou group are of a superior migration channel, and the concealed faults that developed the north of the southern basin margin formed a natural drainage area. Therefore, a complete hydrogeological cycle is formed in the southern basin (Figure 15).

Uranium tends to migrate in alkaline water and precipitate in medium-acidic water,[89] while the southern Yili basin has exactly the favorable hydrogeochemical conditions, with alkaline water in the shallow and medium-weak acidic water in the deep.[90] The shallow water is rich in $HCO_3^-$, which can react with uranium in rocks to form $UO_2(CO_3)_2^{2-}$ and $UO_2(CO_3)_3^{4-}$, which has stable migration ability. When encountering reductants, such as



https://doi.org/10.1021/acsomega.1c06754
ACS Omega 2022, 7, 5453−5470

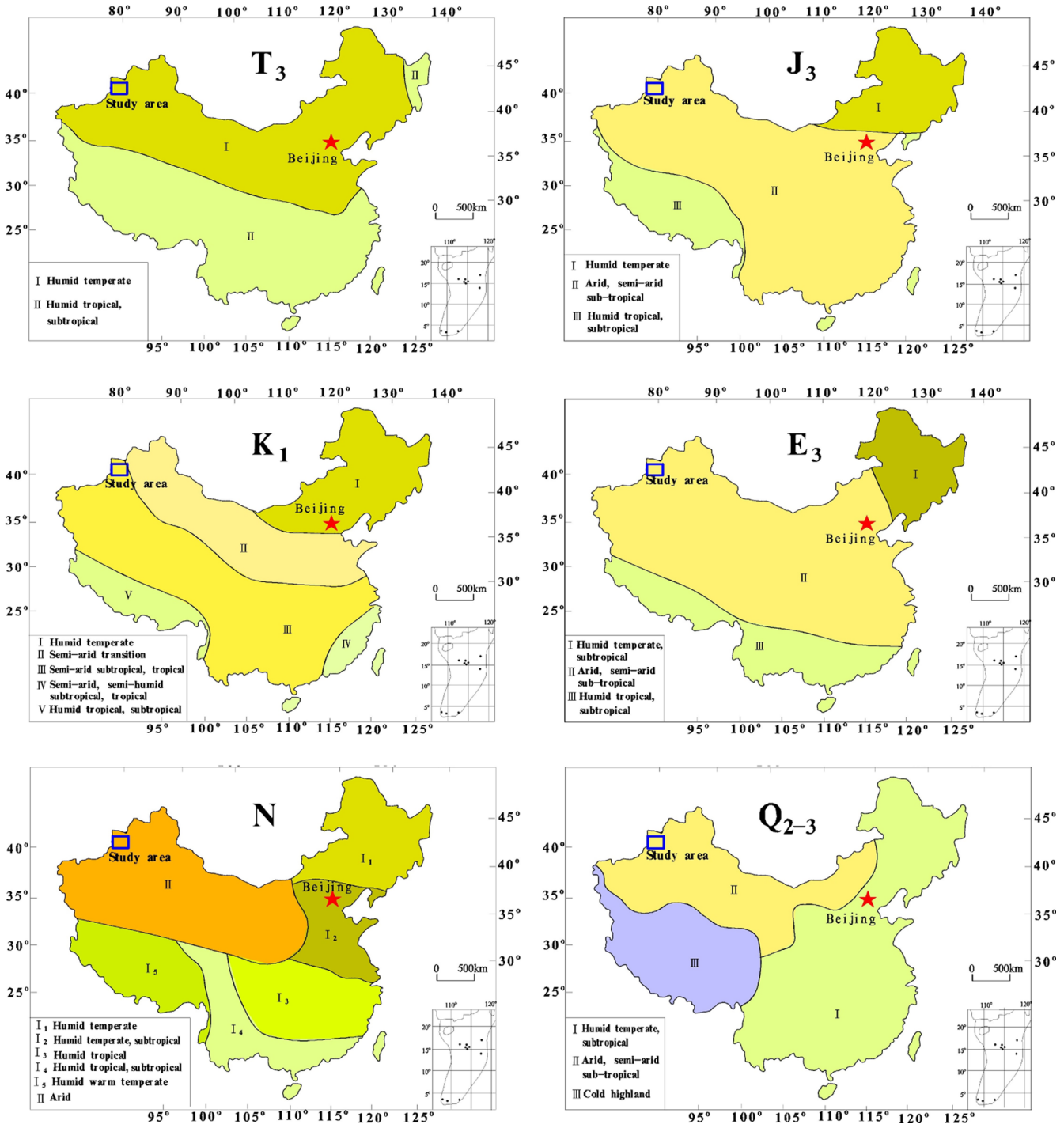


**Figure 16.** Climate evolution since the Triassic in China (modified from ref 92).

coal seam, oil and gas, and pyrite, it leads to uranium precipitation and enrichment.[4] The main reaction equation is as follows

$$2C + SO_4^{2-} + 2H_2O = H_2S + 2CO_2 + 2OH^- \quad (1)$$

$$CH_4 + SO_4^{2-} = H_2S + CO_3^{2-} + H_2O \quad (2)$$

$$Fe_2O_3 + 4H_2S = 2FeS_2 + 3H_2O + 2H^+ \quad (3)$$

$$4UO_2(CO_3)_3^{4-} + H_2S + 12H_2O = 4UO_2 \downarrow + 8H_2O + 12CO_3^{2-} + SO_4^{2-} + 10H^+ \quad (4)$$

$$15UO_2(CO_3)_3^{4-} + 2FeS_2 + 52H_2O = 15UO_2 \downarrow + 30H_2O + 2Fe(OH)_3 + 4SO_4^{2-} + 45CO_3^{2-} + 38H^+ \quad (5)$$

*3.2.5. Paleoclimate.* Overall, the Yili basin had humid and warm climate in the Triassic and early-middle Jurassic, then it changes to an arid or semi-arid paleoclimate since the late



https://doi.org/10.1021/acsomega.1c06754
ACS Omega 2022, 7, 5453−5470

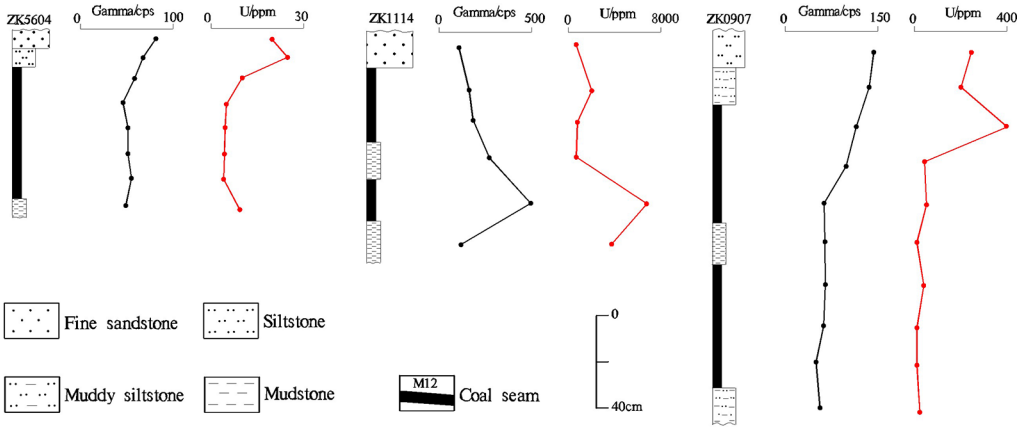


**Figure 17.** Uranium mineralization occurs at the interface between the sandstone and coal seam in the Honghaigou uranium mine.

**Table 7. Relationship between Uranium and Organic Carbon, Total Sulfur, and Valence Iron of the Interlayer Oxidation Zone in the Yili Basin (from Refs 18 19, and 94)**

| mining area | stratum | redox conditions | $U$ ($10^{-6}$) | $C_{org}$ (%) | $S_t$ (%) | $Fe^{2+}$ (%) | $Fe^{3+}/Fe^{2+}$ |
|---|---|---|---|---|---|---|---|
| Honghaigou | Toutunhe | oxidizing zone | 10.5 | 0.09 | 0.02 | 0.22 | 4.2 |
| | | intermediate zone | 62.08 | 0.6 | 0.68 | 0.53 | 2.51 |
| | | reduction zone | 15.8 | 0.49 | 0.48 | 0.44 | 1.92 |
| | Xishanyao | oxidizing zone | 3.71 | 0.09 | 8.66 | 0.11 | 1.08 |
| | | intermediate zone | 544.26 | 0.58 | 1.46 | 0.43 | 0.63 |
| | | reduction zone | 5.65 | 0.27 | 0.57 | 0.65 | 0.37 |
| Zhajisitan | Sangonghe | oxidizing zone | 3.8 | 0.06 | 0.07 | nd | nd |
| | | intermediate zone | 47.4−212.7 | 0.46−0.64 | 0.27−0.28 | nd | nd |
| | | reduction zone | 5.7 | 0.31 | 0.2 | nd | nd |

Jurassic (Figure 16). In early-moderate Jurassic in the Yili basin, it was warm and the vegetation was flourishing. Meanwhile, the tectonic movement brought about a fill and level up sedimentary feature in the basin since the Miocene, resulting in the huge thick dark coal-bearing formation of the Shuixigou group in the Jurassic system. The formation is characterized by a large number of coal seams, high organic matter content in non-coal strata, and extensive development of the braided river delta and sedimentary fan-braided river depositional system. It not only provides a good channel and storage space for the migration of uranium-bearing oxidized water but also provides a reductant necessary for uranium enrichment.

In the late Jurassic, the climate was gradually dry, resulting in the variegated clastic formation. In the Cretaceous, the climate was the most arid, leading to the formation of red clastic formation. Since the Cenozoic, an arid and semi-arid climate had gradually formed, vegetation was not developed, and the humus layer was thin, which was conducive to the infiltration of atmospheric oxygen into the interlayer oxidation zone. At the same time, the evaporation led to uranium enrichment in groundwater, so that the interlayer oxidation zone developed continuously toward the basin and generated uranium mineralization.[13−15,91]

*3.2.6. Reductant.* In uraniferous water, uranium is mostly transported in the form of uranyl ions between layers in the sand body. When encountering with the reductant, such as coal seam, oil and gas, pyrite and organic carbon in the strata, the Eh value of water medium will be sharply cut down. As has been described in Section 3.2.4, uranium is reduced from a hexavalent to a tetravalent with the destruction of uranyl ions, gradually precipitated, and enriched.[93] Therefore, uranium mineralization in the Yili basin is usually located in the contact zone between the sand body and coal seam or at the top of the coal seam beneath the sandstone (Figure 17), which is direct evidence of the reduction and precipitation of uranium by coal. Table 7 shows the relationship between the uranium content and sulfur, organic carbon, and valence iron content.

In addition, the distribution of uranium occurrences in the Yili basin is highly consistent with asphalt and surface oil seedlings. The consistency between the ore-forming ages of most uranium deposits and the neotectonic activity indicates that the tectonic activity revived the deep fault, thus making the reducing fluid such as oil and gas rise along the fault and enter the ore bearing layer. The above reductant prevented the migration of uranium and led to its precipitation and enrichment.[22]

## 4. CONCLUSIONS

(1) Uranium enrichment occurs in both the southern and northern margins of the Yili Basin, and uranium deposits are mainly distributed in the southern margin. Uranium ore bodies and coal seams usually have a certain correlation in the spatial distribution and genesis, which is closely related to coal, oil and gas, pyrite, and other reductants. Host rocks of uranium are mainly middle-coarse sandstone, followed by coal, and occasionally even mudstone. Uranium can occur in either inorganic or organic states, and the latter is sometimes more common. Uranium enrichment to varying degrees can be seen in the strata since the Jurassic, but the Cenozoic is the most important metallogenic period.

(2) Uranium enrichment in coal-bearing strata in the Yili Basin is the overall coupling of the uranium source, structure, deposition, hydrogeology, paleoclimate, and



https://doi.org/10.1021/acsomega.1c06754
ACS Omega 2022, 7, 5453−5470

Table 8. Relationship between Uranium Mineralization and the Coupling of Tectonic Activity, Sedimentation, and Climate (from Refs 22 and 92)

| age | pre-P | P | $T_3$ | $J_3$ | $K_1$ | $E_1$ | N | Q |
|---|---|---|---|---|---|---|---|---|
| structure | basement evolution | strong stretching | | weak stretching | denudation uplift | weak extrusion | neotectonic movement | |
| sedimentation | | conglomerate | yellow conglomerate-gray mudstone | conglomerate, sandstone, mudstone, and coal | red conglomerate-gray mudstone | brown-red sandy conglomerate, sandstone, and mudstone | yellow conglomerate, calcareous mudstone | sand, gravel, clay |
| climate | | arid, semi-arid | semi-arid, semi-humid | humid | arid | arid, semi-arid subtropical | arid | arid, semi-arid |
| uranium mineralization | rich uranium source rocks | | | uranium bearing formation | early interlaminar oxidation mineralization | | late interbedded oxidation mineralization | |

reductant (Table 8). Tectonic activity exposed uranium-rich parent rocks to denudation, leading to the migration of uraniferous fluid along the gentle slope into the basin. Sedimentary formation (of coarse grain and thick sandstone body) provided favorable migration channels for the uraniferous fluid. Paleoclimate transformation (humid to arid) caused evaporation and uranium concentration. When encountered with a structural change of strata (where the thickness of the sand body becomes thinner and the sand body transitions into coal seam or mudstone) or reductants such as coal, hydrocarbon, pyrite, and clay minerals, uranium from the uraniferous fluid was then reduced and precipitated, leading to the formation of uranium deposits.

(3) Tectonic activity may be the dominant factor, which consists of three stages: basement evolution, caprock development, and neotectonic activity transformation. First, the development of uranium-rich strata in the Yili Basin before the Paleozoic, especially the Carboniferous rifting, provided abundant uranium sources. Meanwhile, the weak extensional basin-forming tectonic background of the Jurassic overall controlled the generation of the braided river delta and other favorable sedimentary systems, which formed a favorable storage reservoir and migration channel for uraniferous fluid. In addition, neotectonic movement resulted in the strata slanting in the southern margin of the basin, which led to the uplift and denudation of the uranium-rich parent rock. Consequently, the gentle monocline structure provided quite advantageous hydrodynamic conditions for the migration of uraniferous fluid.

(4) Since the Jurassic, the favorable sedimentary systems such as the braided river delta are relatively developed, which promoted the formation of a favorable reservoir space and migration channel for uraniferous fluid in a weakly extensional tectonic background. The stratigraphic structure of mudstone (coal)-sandstone-mudstone were stable, the sand body were of appropriate thickness (generally 10−30 m) and steady extension, which provided a superb storage reservoir for uranium mineralization.

(5) Paleoclimate in the Jurassic was of drought-semi-arid subtropical, resulting in the lush vegetation, which brought about the formation of a large number of reductants (coal, carbon dust, pyrite, etc.). Since the Cenozoic, arid and semi-arid climate have been favorable to the infiltration of oxygen and concentration of uranium for uraniferous fluid, leading to the continuous development of the interlayer oxidation zone toward the basin center and enrichment of uranium.

## 5. OUTLOOK

**5.1. Resource Development.** Uranium deposits and coal seam have a certain correlation in their genesis and spatial distribution or sometimes uranium deposit develops directly in the coal seam in the Yili basin, which increased the difficulty of the joint development of the two mineral. At present, coal with uranium more than 10 bq/kg are under restricted exploitation in Xianjiang. Meanwhile, uranium mining is mainly based on the in situ leaching method, which inevitably injects a large amount of acid or alkali into the strata. However, coal mining usually



https://doi.org/10.1021/acsomega.1c06754
ACS Omega 2022, 7, 5453−5470

requires drainage, which would make uranium mining impossible or difficult, and vice versa.

In the future, it is possible to strengthen the study on the physical chemistry of the ore-bearing host rock and the occurrence state of uranium, on the basis of which underground in situ gasification and leaching, could be implemented, improved, and popularized. That is, to gasify coal underground and to leach uranium from the coal ash and brought them to the surface as fluid (gas or liquid). In addition, coal and uranium exploration are managed by two organizations in China. Therefore, to strengthen the cooperation and coordination and to share geological data between the two organization will greatly improve exploration efficiency and reduce costs.

**5.2. Environmental Protection.** Sandstone uranium mining will inject a large amount of acid or alkali into the underground aquifer, resulting in acid and alkali pollution. Meanwhile, the leached uranium will enter the groundwater circulation, resulting in uranium levels in the hair and urine of exposed subjects several times higher than those of the unexposed.[95−98] The accumulation of high-uranium sandstone, coal, and coal ash on the surface may be up to the level of solid radiation, leading to the absorbed dose rate of $\gamma$ radiation in the air to be tens of times higher than the average level.[99]

It is of great significance to strengthen the study of the occurrence state of uranium in the ore (especially uranium in coal), improve the mining method of the uranium ore in coal-bearing rock series, and explore the method of coal and uranium separation in the preparation of uranium-rich coal and the fixation of uranium in the combustion process, so as to reduce environmental hazards.

## AUTHOR INFORMATION


### Corresponding Author

**Wenfeng Wang** − *School of Resources and Geosciences, China University of Mining and Technology, Xuzhou 221116, China; Key Laboratory of Coalbed Methane Resources and Reservoir Formation Process of the Ministry of Education, China University of Mining and Technology, Xuzhou 221000, China; School of Geology and Mining Engineering, Xinjiang University, Urumqi 830047, China;* orcid.org/0000-0002-2200-0250; Email: wangwenfeng@cumt.edu.cn

### Authors

**Hongyang Bai** − *School of Resources and Geosciences, China University of Mining and Technology, Xuzhou 221116, China; Key Laboratory of Coalbed Methane Resources and Reservoir Formation Process of the Ministry of Education, China University of Mining and Technology, Xuzhou 221000, China*

**Qingfeng Lu** − *School of Resources and Geosciences, China University of Mining and Technology, Xuzhou 221116, China; Key Laboratory of Coalbed Methane Resources and Reservoir Formation Process of the Ministry of Education, China University of Mining and Technology, Xuzhou 221000, China;* orcid.org/0000-0003-3282-0276

**Wenlong Wang** − *School of Resources and Geosciences, China University of Mining and Technology, Xuzhou 221116, China; Key Laboratory of Coalbed Methane Resources and Reservoir Formation Process of the Ministry of Education, China University of Mining and Technology, Xuzhou 221000, China*

**Shuo Feng** − *School of Geology and Mining Engineering, Xinjiang University, Urumqi 830047, China*

**Bofei Zhang** − *School of Resources and Geosciences, China University of Mining and Technology, Xuzhou 221116, China; Key Laboratory of Coalbed Methane Resources and Reservoir Formation Process of the Ministry of Education, China University of Mining and Technology, Xuzhou 221000, China*

Complete contact information is available at: https://pubs.acs.org/10.1021/acsomega.1c06754


### Notes

The authors declare no competing financial interest.

## ACKNOWLEDGMENTS

This study was supported by the National Natural Science Foundation of China (nos. U1903207 and 41972176), Postgraduate Research & Practice Innovation Program of the Jiangsu Province (grant KYCX21_2321), Open Fund project of Key Laboratory of Coal Measure Mineral Resources of China National Administration of Coal Geology (KFKT-2020-2), and a Project Funded by the Priority Academic Program Development of Jiangsu Higher Education Institutions. We thank the Nuclear Industry 216 Geological Team for their supports in field work. We appreciate the anonymous reviewers for their constructive comments.

## REFERENCES


(1) China Power Media Energy Information Research Center. *China Energy Big Data Report (2021)-Energy Complex*: Beijing, 2021; pp 1−95. (in Chinese).

(2) China Nuclear Energy Industry Association. *China Nuclear Energy Development Report 2021*: Beijing, 2021; pp 1−198. (in Chinese).

(3) Finch, W. I.; Davis, J. F. Sandstone-type uranium deposits-an introduction. *Geological Environments of Sandstone Type Uranium Deposits, TECDOC-328*; IAEA: Vienna, 1985; pp 11−20.

(4) Zhang, C.; Liu, H. A growing sandstone type uranium district in South Yili Basin, NW China as a result of extension of Tien Shan Orogen: Evidences from geochronology and hydrology. *Gondwana Res.* **2019**, *76*, 146−172.

(5) Zhang, J. Innovation and development of metallogenic theory for sandstone type uranium deposit in China. *Uranium Geol.* **2016**, *32*, 321−332. (in Chinese with English abstract)

(6) Cai, Y.; Zhang, J.; Li, Z.; Guo, Q.; Song, J.; Fan, H.; Liu, W.; Qi, F.; Zhang, M. Outline of uranium resources characteristics and metallogenetic regularity in China. *Acta Geol. Sin.* **2015**, *89*, 918−937 (in Chinese with English abstract).

(7) Cuney, M. The extreme diversity of uranium deposits. *Miner. Deposita* **2009**, *44*, 3−9.

(8) Cuney, M.; Kyser, K. Recent and not-so-recent developments in uranium deposits and implications for exploration. *Mineral. Assoc. Can., Short Course Ser.* **2009**, *39*, 210−250.

(9) Dahlkamp, J. F. *Uranium Deposits of the World*; Springer: Berlin Heidelberg, 2009; pp 1−30.

(10) Zhang, C.; Yi, C.; Dong, Q.; Cai, Y.-Q.; Liu, H.-X. Geological and geochronological evidence for the effect of Paleogene and Miocene uplift of the Northern Ordos Basin on the formation of the Dongsheng uranium district, China. *J. Geodyn.* **2018**, *114*, 1−18.

(11) Ding, B.; Liu, H.; Zhang, C.; Liu, H.; LI, P.; Zhang, B. Mineralogy, Fluid Inclusion and H-O-C-S Stable Isotopes of Mengqiguer Uranium Deposit in the Southern Yili Basin, Xinjiang: Implication for Ore Formation. *Acta Geol. Sin. (Engl. Ed.)* **2020**, *94*, 1488−1503.

(12) Cheng, X. *Geological Characteristics and Genetic analysis of Sandstone Uranium Deposits in Wukuerqi-Mongqiguer AreaSouthern Margin of Yili Basin*; Northwest University: Xi'an, 2019; pp 1−76. (in Chinese with English abstract).

(13) Wang, M.; Li, H.; Qiu, Y. Coal-type uranium metallogenic analysis in Honghaigou area, Yili Basin, Xinjiang. *Coal Geol. Chin.* **2015**, *27*, 12−16. (in Chinese with English abstract)

(14) Zhong-ming, A.; Xin-ke, Z. The mechanism of multi-layer ore-forming of Daladi uranium deposit in the Yili Basin, and its inspiration significance for uranium prospecting. *Xinjiang Geol.* **2003**, *21*, 433−436. (in Chinese with English abstract)
(15) Wang, J.; Geng, S. F. Characteristics of the interlayer oxidation zone and the Kujieertai uranium deposit in Yili Basin. *Chin. Geol.* **2009**, *36*, 705−713. (in Chinese with English abstract)
(16) Wang, J.; Min, M.; Chen, H.; He, Y.; Gao, L. Petrological and geochemical characteristics of Shuixigou Group in Yili Basin. *Uranium Geol.* **2003**, *19*, 8−15. (in Chinese with English abstract)
(17) Jia, Z.; Zhang, H.; Chen, W.; Zhang, L.; Qiu, Y. Ore-control factors of Honghaigou coal type uranium deposit in the southern margin of Yili Basin, Xinjiang. *Miner. Explor.* **2020**, *11*, 2417−2423. (in Chinese with English abstract)
(18) Fenxiong, C.; Fengjun, N.; Chengyong, Z.; Zhanfeng, Z. Distribution characteristics of interlayer oxidation zone and its main controlling factors of upper xishanyao formation in honghaigou area,Yili Basin. *Geol. Sci. Technol. Inf.* **2016**, *35*, 105−111. (in Chinese with English abstract)
(19) Chen, F.; Nie, F.; Zhang, C.; Zhang, Z. Geological characteristics and genetic mechanism of the Honghaigou uranium deposit in the southern margin of Yili Basin. *Acta Geol. Sin.* **2016**, *090*, 3324−3336. (in Chinese with English abstract)
(20) Wang, J.; Min, M.; Chen, Y.; Peng, X. Study on the relationship between $SiO_2/Al2O_3$ ratios and oreebearing capacity in interstratified oxidized zone: exemplified by Kujie'ertai and Wukuerqi uranium deposit. *Geol. J. China Univ.* **2005**, *11*, 77−84. (in Chinese with English abstract)
(21) Wang, J.; Min, M.; Peng, X.; Chen, Y.; University, N.; Zhu, X. Preliminary discussion on the activity of major elements in Kujiertai uranium deposit, Yili Basin. *Geol. Rev.* **2005**, *51*, 143−150. (in Chinese with English abstract)
(22) Li, S.; Ou, G.; Han, X.; Cai, Y.; Zheng, E.; Li, X. Study on the relationship between oil-gas and ore-formation of the in-situ leachable sandstone-type uranium deposit in Yili Basin. *Acta Geol. Sin.* **2006**, *80*, 118−124. (in Chinese with English abstract)
(23) Han, B.-F.; He, G.-Q.; Wang, X.-C.; Guo, Z.-J. Late Carboniferous collision between the Tarim and Kazakhstan-Yili terranes in the western segment of the South Tian Shan Orogen, Central Asia, and implications for the Northern Xinjiang, western China. *Earth-Sci. Rev.* **2011**, *109*, 74−93.
(24) Biske, Y. S.; Seltmann, R. Paleozoic Tian-Shan as a transitional region between the Rheic and Urals-Turkestan oceans. *Gondwana Res.* **2010**, *17*, 602−613.
(25) Glorie, S.; De Grave, J.; Buslov, M. M.; Elburg, M. A.; Stockli, D. F.; Gerdes, A.; Van den haute, P. Multi-method chronometric constraints on the evolution of the Northern Kyrgyz Tien Shan granitoids (Central Asian Orogenic Belt): from emplacement to exhumation. *J. Asian Earth Sci.* **2010**, *38*, 131−146.
(26) Gao, J.; Long, L.; Klemd, R.; Qian, Q.; Liu, D.; Xiong, X.; Su, W.; Liu, W.; Wang, Y.; Yang, F. Tectonic evolution of the South Tianshan orogen and adjacent regions, NW China: geochemical and age constraints of granitoid rocks. *Int. J. Earth Sci.* **2009**, *98*, 1221−1238.
(27) Sun, J.; Li, Y.; Zhang, Z.; Fu, B. Magnetostratigraphic data on Neogene growth folding in the foreland basin of the southern Tianshan Mountains. *Geology* **2009**, *37*, 1051−1054.
(28) Konopelko, D.; Biske, G.; Seltmann, R.; Kiseleva, M.; Matukov, D.; Sergeev, S. Deciphering Caledonian events: timing and geochemistry of the Caledonian magmatic arc in the Kyrgyz Tien Shan. *J. Asian Earth Sci.* **2008**, *32*, 131−141.
(29) De Grave, J.; Buslov, M. M.; Van den haute, P. Distant effects of India-Eurasia convergence and Mesozoic intracontinental deformation in Central Asia: Constraints from apatite fission-track thermochronology. *J. Asian Earth Sci.* **2007**, *29*, 188−204.
(30) Charreau, J.; Chen, Y.; Gilder, S.; Dominguez, S.; Avouac, J.-P.; Sen, S.; Sun, D.; Li, Y.; Wang, W.-M. Magnetostratigraphy and rock magnetism of the Neogene Kuitun He section (northwest China): implications for Late Cenozoic uplift of the Tianshan mountains. *Earth Planet. Sci. Lett.* **2005**, *230*, 177−192.
(31) Charreau, J.; Gilder, S.; Chen, Y.; Dominguez, S.; Avouac, J.-P.; Sen, S.; Jolivet, M.; Li, Y.; Wang, W. Magnetostratigraphy of the Yaha section, Tarim Basin (China): 11 Ma acceleration in erosion and uplift of the Tian Shan mountains. *Geology* **2006**, *34*, 181−184.
(32) Min, M.; Xu, H.; Chen, J.; Fayek, M. Evidence of uranium biomineralization in sandstone-hosted roll-front uranium deposits, northwestern China. *Ore Geol. Rev.* **2005**, *26*, 198−206.
(33) Abdrakhmatov, K. Y.; Aldazhanov, S. A.; Hager, B. H.; Hamburger, M. W.; Herring, T. A.; Kalabaev, K. B.; Makarov, V. I.; Molnar, P.; Panasyuk, S. V.; Prilepin, M. T.; Reilinger, R. E.; Sadybakasov, I. S.; Souter, B. J.; Trapeznikov, Y. A.; Tsurkov, V. Y.; Zubovich, A. V. Relatively recent construction of the Tien Shan inferred from GPS measurements of present-day crustal deformation rates. *Nature* **1996**, *384*, 450−453.
(34) Hendrix, M. S.; Dumitru, T. A.; Graham, S. A. Late Oligocene-early Miocene unroofing in the Chinese Tian Shan: An early effect of the India-Asia collision. *Geology* **1994**, *22*, 487−490.
(35) Avouac, J. P.; Tapponnier, P.; Bai, M.; You, H.; Wang, G. Active thrusting and folding along the northern Tien Shan and late Cenozoic rotation of the Tarim relative to Dzungaria and Kazakhstan. *J. Geophys. Res.: Solid Earth* **1993**, *98*, 6755−6804.
(36) Wang, B.; Faure, M.; Cluzel, D.; Shu, L.; Charvet, J.; Meffre, S.; Ma, Q. Late Paleozoic tectonic evolution of the northern West Chinese Tianshan Belt. *Geodin. Acta* **2006**, *19*, 237−247.
(37) Wang, B.; Chen, Y.; Zhan, S.; Shu, L.; Faure, M.; Cluzel, D.; Charvet, J.; Laurent-Charvet, S. Primary Carboniferous and Permian paleomagnetic results from the Yili Block (NW China) and their implications on the geodynamic evolution of Chinese Tianshan belt. *Earth Planet. Lett.* **2007**, *263*, 288−308.
(38) Wang, B.; Shu, L. S.; Cluzel, D.; Faure, M.; Charvet, J. Geochemical constraints on Carboniferous volcanic rocks of the Yili Block (Xinjiang, NW China): Implication for the tectonic evolution of Western Tianshan. *J. Asian Earth Sci.* **2007**, *29*, 148−159.
(39) Li, S.; Han, X.; Cai, Y.; Huang, J.; Cai, G. Metallogenic model and prospecting targets for interlayer oxidation type sandstone-hosted uranium deposits in intermountain basins of the Tianshan orogenic belt. *Miner. Deposits* **2006**, *25*, 241−244. (in Chinese)
(40) Chen, C.; Lu, H.; Jia, D.; Cai, D.; Wu, S. Closing history of the southern Tianshan oceanic basin, western China: an oblique collisional orogeny. *Tectonophysics* **1999**, *302*, 23−40.
(41) Allen, M. B.; Windley, B. F.; Zhang, C. Palaeozoic collisional tectonics and magmatism of the Chinese Tien Shan, Central Asia. *Tectonophysics* **1993**, *220*, 89−115.
(42) Enkin, R. J.; Chen, Y.; Courtillot, V.; Besse, J.; Xing, L.; Zhang, Z.; Zhuang, Z.; Zhang, J. A Cretaceous pole from south China, and the Mesozoic hairpin turn of the Eurasian apparent polar wander path. *J. Geophys. Res.* **1991**, *96*, 4007−4027.
(43) Min, M.; Chen, J.; Wang, J.; Wei, G.; Fayek, M. Mineral paragenesis and textures associated with sandstone-hosted roll-front uranium deposits, NW China. *Ore Geol. Rev.* **2005**, *26*, 51−69.
(44) Li, S.; Han, X.; Cai, Y.; Zheng, E.; Wang, B. Depositional system of the lower-middle jurassic shuixigou group in the western segment of the southern margin of the Yili basin and its controls on uranium mineralization. *Chin. Geol.* **2006**, *33*, 582−590. (in Chinese with English abstract)
(45) Bonnetti, C.; Cuney, M.; Malartre, F.; Michels, R.; Liu, X.; Peng, Y. The Nuheting Deposit, Erlian Basin, NE China: synsedimentary to diagenetic uranium mineralization. *Ore Geol. Rev.* **2015**, *69*, 118−139.
(46) Bonnetti, C.; Cuney, M.; Bourlange, S.; Deloule, E.; Poujol, M.; Liu, X.; Peng, Y.; Yang, J. Primary uranium sources for sedimentary-hosted uranium deposits in NE China: insight from basement igneous rocks of the Erlian Basin. *Miner. Deposita* **2017**, *52*, 297−315.
(47) Bonnetti, C.; Liu, X.; Zhaobin, Y.; Cuney, M.; Michels, R.; Malartre, F.; Mercadier, J.; Cai, J. Coupled uranium mineralisation and bacterial sulphate reduction for the genesis of the Baxingtu sandstone-hosted U deposit, SW Songliao Basin, NE China. *Ore Geol. Rev.* **2017**, *82*, 108−129.
(48) Seltmann, R.; Konopelko, D.; Biske, G.; Divaev, F.; Sergeev, S. Hercynian post-collisional magmatism in the context of Paleozoic


https://doi.org/10.1021/acsomega.1c06754
*ACS Omega* 2022, 7, 5453−5470

magmatic evolution of the Tien Shan orogenic belt. *J. Asian Earth Sci.* **2011**, *42*, 821−838.
(49) Li, J. L.; Qian, Q.; Gao, J.; Su, W.; Zhang, X.; Liu, X.; Jiang, T. Geochemistry, zircon U-Pb ages and tectonic settings of the Dahalajunshan volcanics and granitic intrusions from the Adengtao area in the southeast Zhaosu, western Tianshan mountains. *Acta Petrol. Sin.* **2010**, *26*, 2913−2924. (in Chinese with English abstract)
(50) Konopelko, D.; Biske, G.; Seltmann, R.; Eklund, O.; Belyatsky, B. Hercynian post-collisional A-type granites of the Kokshaal Range, Southern Tien Shan, Kyrgyzstan. *Lithos* **2007**, *97*, 140−160.
(51) Barbarin, B. A review of the relationships between granitoid types, their origins and their geodynamic environments. *Lithos* **1999**, *46*, 605−626.
(52) Zhang, G.; Li, S.; Liu, J.; Teng, Z.; Jin, H.; Li, W.; Huang, X.; Wu, Y. Structural feature and evolution of Yili Basin, Xinjiang. *Earth Sci. Front.* **1999**, *6*, 203−214. (in Chinese with English abstract)
(53) Wang, Y.; Chen, Z.; Liu, J.; Zheng, E.; Wang, C.; Li, S.; Han, X. Neotectonics in southern Yili Basin and its control of sandstone-type uranium deposits. *Geotect. Metallogenia* **2006**, *30*, 486−494. (in Chinese with English abstract)
(54) Wang, Z.; Li, Z.; Guan, T.; Zhang, G. Geological characteristics and metallogenic mechanism of No.511 Sandstone type uranium ore deposit in Yili Basin, Xinjiang. *Miner. Deposits* **2006**, *25*, 302−311. (in Chinese with English abstract)
(55) Li, S. *The Enrichment Characteristic and Accumulation Conditions Analysis of Various Energy Resources in the Lower Middle Jurassic, in Yili Basin*; Chengdu University of Technology: Chengdu, 2019; pp 1−118. (in Chinese with English abstract).
(56) Chen, D.; Wang, R.; Li, S.; Zhang, K. *Metallogenic Geologic Conditions and Prospecting Direction of Sanddtone Type Uranium Mineralizations in Yili Basin of Xinjiang*; China Nuclear Science and Technology Report, 1994; pp 824−837. (in Chinese).
(57) Li, S.; Chen, H.; Zhou, J.; Wang, M.; Liu, J.; Wang, B. Source Convergence Process and its Restriction on Sandstone Type Uranium Metallization-A Case Study of Mengqiguer Uranium Deposit in the Southern Margin of Yili Basin, Xinjiang. *Uranium Geol.* **2016**, *32*, 137−145. (in Chinese with English abstract)
(58) Min, M.-Z.; Luo, X.-Z.; Mao, S.-L.; Wang, Z.-Q.; Wang, R. C.; Qin, L.-F.; Tan, X.-L. An excellent fossil wood cell texture with primary uranium minerals at a sandstone-hosted roll-type uranium deposit, NW China. *Ore Geol. Rev.* **2001**, *17*, 233−239.
(59) Xia, Y.; Lin, J.; Hou, Y.; Liu, H.; Fan, G. Characteristics of isotope geology of sandstone-type uranium deposit in Yili Basin, Xinjiang. *Uranium Geol.* **2002**, *18*, 150−154. (in Chinese with English abstract)
(60) Zhang, Z.; Jiang, H.; Wang, M. Metallogenic driving factors of Mengqiguer uranium deposit and their significance in prospecting practice in Yili Basin. *Miner. Deposits* **2010**, *29*, 165−166. (in Chinese)
(61) Li, P.; Liu, H. X.; Ding, B.; Tian, M. M. The Zircon U-Pb geochronology and dynamics mechanism for the formation of monzonitic granite in the Qiongbola area, south of Yili Basin. *Chin. Geol.* **2018**, *45*, 720−739. (in Chinese with English abstract)
(62) Liu, W.; Jia, L. Mineralization of daladi uranium - bearing coal deposit. *Acta Mineral. Sin.* **2011**, *S1*, 271−272. (in Chinese)
(63) Li, X. Characteristics of sandstone-type uranium mineralization and ore-controlling factors in Wukurqi ore district at southern margin of Yili Basin, Xinjiang. *Uranium Geol.* **2002**, *18*, 28−35. (in Chinese with English abstract)
(64) Suo, S. *Research on Metallogenic Characteristics and Ore-controlling Factors of Mengqiguer Uranium Deposit*; East China University of Technology: Nanchang, 2013; pp 1−53. (in Chinese with English abstract).
(65) Jiang, W.; Wang, C.; Yong, L.; Chao, H.; Shi, X. Petrological characteristics of middle and lower Jurassic sandstone in the southern margin of Yili Basin and the indicative significance for provenance analysis. *J. East China Univ. Sci. Technol., Nat. Sci. Ed.* **2018**, *41*, 307−314. (in Chinese with English abstract)
(66) Dong, Y.; Nie, F.; Zhang, C.; Zhang, H. Study on sandstone petrologic feature of the toutunhe formation and its controls on uranium enrichment in honghaigou area, Yili Basin. *Sci. Technol. Eng.* **2016**, *016*, 9−15. (in Chinese with English abstract)
(67) Harshman, E. N. *Distribution of Elements in Some of Roll Type Uranium Deposits in Formation of Uranium Ore Deposits*; IAEA: Vienna, 1974; pp 163−183.
(68) Hostetler, P. B.; Garrels, R. M. Transportation and precipitation of uranium and vanadium at low temperatures, with special reference to sandstone-type uranium deposits. *Econ. Geol.* **1962**, *57*, 137−167.
(69) Zhang, Y.; Li, S.; Wang, G.; Li, S.; Chen, F.; Zheng, E. REE geochemistry of sandstone-type uranium deposit in interlayer zone in the southern margin of Yili Basin, Xinjiang. *Geochimica* **2006**, *35*, 211−218. (in Chinese with English abstract)
(70) Dai, S.; Yang, J.; Ward, C. R.; Hower, J. C.; Liu, H.; Garrison, T. M.; French, D.; O'Keefe, J. M. K. Geochemical and mineralogical evidence for a coal-hosted uranium deposit in the Yili Basin, Xinjiang, northwestern China. *Ore Geol. Rev.* **2015**, *70*, 1−30.
(71) Yang, J. Concentration and distribution of uranium in chinese coals. *Energy* **2007**, *32*, 203−212.
(72) Cun, X. *Metallogenic Chronology and its Geological Significance in Nalinggou Sandstone-type uranium, Ordos Basin*; Northwest University: Xi'an, 2016; pp 1−70. (in Chinese with English abstract).
(73) Song, Z. *Metallogenic Chronology and its Geological Significance in Hangjinqi Sandstone-type uranium, Ordos Basin*; Northwest University: Xi'an, 2013; pp 1−75. (in Chinese with English abstract).
(74) Xiang, W.; Chen, X.; Pang, Y.; Fang, X.; Li, T. Mineralogical and geochemical characteristics and genetic mechanism ofgray-greenish alteration sandstone of the Dongsheng uranium deposit in the Ordos basin, North China. *Miner. Deposits* **2006**, *25*, 261−264. (in Chinese with English abstract)
(75) Xia, Y.; Lin, J.; Liu, H.; Fang, J.; Hou, Y. Research on geochronology of sandstone-hosted uranium ore-formation in major uranium-productive basins, Northern China. *Uranium Geol.* **2003**, *19*, 129−136. (in Chinese with English abstract)
(76) Ding, B.; Liu, H.; Li, P.; Jiang, H.; Zhang, H.; Zhang, B. The genetic mechanism of kaolinte in ore-bearing sandstone in the Mengqiguer uranium deposit, Yili, and its relation with uranium mineralization. *Acta Geol. Sin.* **2019**, *93*, 2020−2036. (in Chinese with English abstract)
(77) Wronkiewicz, D. J.; Condie, K. C. Geochemistry of Archean shales from the Witwatersrand Supergroup, South Africa: source-area weathering and provenance. *Geochim. Cosmochim. Acta* **1987**, *51*, 2401−2416.
(78) Mclennan, S. M. Weathering and Global Denudation. *J. Geol.* **1993**, *101*, 295−303.
(79) Jiang, W. *The Provenance Analysis of Jurassic and Its Relation to Basin and Mountain in the Southern Margin of Yili Basin, Xinjiang*; Chengdu University of Technology: Chengdu, 2017; pp 1−96. (in Chinese with English abstract).
(80) Girty, G. H.; Ridge, D. L.; Knaack, C.; Johnson, D.; Al-Riyami, R. K. Provenance and depositional setting of Paleozoic chert and argillite, Sierra Nevada, California. *J. Sediment. Res.* **1996**, *66*, 107−118.
(81) Floyd, P. A.; Leveridge, B. E. Tectonic environment of the Devonian Gramscatho basin, south Cornwall: framework mode and geochemical evidence from turbiditic sandstones. *J. Geol. Soc.* **1987**, *144*, 531−542.
(82) Taylor, S. R.; McLennan, S. M. *The Continental Crust: Its Composition and Evolution*; Blackwell: London, 1985; pp 1−312.
(83) Huang, G. *The Mineral Composition Debris Source Tracer Study of Mengqiguer Uraniumdeposit in Yili Basin*; East China University of Technology: Nanchang, 2017; pp 1−63. (in Chinese with English abstract).
(84) Zhang, H.; Nie, F.; Rao, M.; Wang, G.; Zhang, Z. Lithology characteristics of the uranium-bearing sandstone in the Shuixigou group in the Mengqiguer area of the Yili Basin and their implications. *Geol. Explor.* **2012**, *48*, 132−139. (in Chinese with English abstract)
(85) Hou, M.; Jiang, W.; Ni, S.; Huang, H.; Luo, W.; Shi, X.; Miu, Z. Geochemical characteristic of the lower and middle Jurassic clastic rocks in the southern margin of the Yili Basin, Xinjiang and its


https://doi.org/10.1021/acsomega.1c06754
*ACS Omega* 2022, 7, 5453−5470

constraints on provenance. *Acta Geol. Sin.* **2016**, *90*, 3337−3351. (in Chinese with English abstract)
(86) Qiu, Y.; Du, M.; Wang, Q.; Yang, J.; Sun, X. Controlling effect of sedimentation to the mineralization of inter-layer oxidation zone sandstone type uranium deposit in the southern margin of Yili Basin. *Mod. Min.* **2017**, *33*, 40−45. (in Chinese with English abstract)
(87) Li, S. Study on the characteristics of sandstone type uranium mineralization leached in situs and its space distribution rule. *Journal of east China geological institute* **1996**, *19*, 332−339. (in Chinese with English abstract)
(88) He, Y.; Rong, H.; Huang, K.; Peng, H.; Wang, J. Hydrogeochemistry characteristics and uranium metallogenic conditions of the groundwater in Yili Basin. *Saf. Environ. Eng.* **2019**, *26*, 725−813. (in Chinese with English abstract)
(89) Shi, W. *Principles of Uranium Hydrogeochemistry*; Atomic Energy Press: Beijing, 1990; pp 1−442. (in Chinese).
(90) Xing, D.; Kang, Y.; Wang, B.; Qiu, Y.; Zhang, H. Main ore-bearing aquifer and hydrogeochemical characteristics of the uranium depositin honghaigou area,southern margin of Yili Basin. *Xinjiang Geol.* **2014**, *32*, 240−243. (in Chinese with English abstract)
(91) Yan, W.; Zhao, Z.; Li, W. Summary of metallogenic geological characteristics of "Kujiertai" sandstone type uranium deposit in Yili Basin. *Sichuan Nonferrous Metals* **2019**, *04*, 27−30. (in Chinese with English abstract)
(92) Dai, S.; Zhang, M.; Peng, D.; Wang, H.; Wu, M.; Chen, R. The Mesozoic-cenozoic Evolution of the Tectonic and Climatic Patterns,nw China. *Mar. Geol. Quat. Geol.* **2013**, *33*, 153 (in Chinese with English abstract).
(93) Zhang, Z. *Uranium Geochemistry*; Atomic Energy Press: Beijing, 1984; pp 1−403. (in Chinese).
(94) Zhongming, A. Analysis on ore-controlling factors of Zhajistan uranium deposit, Xinjiang. *Uranium Geol.* **2000**, *16*, 136−142. (in Chinese with English abstract)
(95) Wufuer, R.; Song, W.; Zhang, D.; Pan, X.; Gadd, G. M. A survey of uranium levels in urine and hair of people living in a coal mining area in Yili, Xinjiang, China. *J. Environ. Radioact.* **2018**, *189*, 168−174.
(96) Chen, J.; Chen, P.; Yao, D.; Huang, W.; Tang, S.; Wang, K.; Liu, W.; Hu, Y.; Zhang, B.; Sha, J. Abundance, distribution, and modes of occurrence of uranium in chinese coals. *Minerals* **2017**, *7*, 239.
(97) Chen, J.; Chen, P.; Yao, D.; Huang, W.; Tang, S.; Wang, K.; Liu, W.; Hu, Y.; Li, Q.; Wang, R. Geochemistry of uranium in Chinese coals and the emission inventory of coal-fired power plants in China. *Int. Geol. Rev.* **2018**, *60*, 621−637.
(98) Juliao, L. M. Q. C.; Melo, D. R.; Sousa, W. O.; Santos, M. S.; Fernandes, P. C.; Godoy, M. Exposure of workers in a mineral processing industry in Brazil. *Radiat. Prot. Dosim.* **2007**, *125*, 513.
(99) Di, S. Analysis on the radiation environment of coal mining associated uranium in Xinjiang. *Arid Environ. Monit.* **2006**, *20*, 149−152. (in Chinese with English abstract)


https://doi.org/10.1021/acsomega.1c06754
*ACS Omega* 2022, 7, 5453−5470